

# Aspects of Quasi-Phasestructure of the Schwinger Model on a Cylinder with Broken Chiral Symmetry

Stephan Dürr

*University of Washington*  
*Particle Theory Group, Box 351560*  
*Seattle, WA 98195 (U.S.A.)*  
durr@phys.washington.edu

arXiv:hep-th/9805124v1 19 May 1998

## Abstract

We consider the  $N_f$ -flavour Schwinger Model on a thermal cylinder of circumference  $\beta = 1/T$  and of finite spatial length  $L$ . On the boundaries  $x^1 = 0$  and  $x^1 = L$  the fields are subject to an element of a one-dimensional class of bag-inspired boundary conditions which depend on a real parameter  $\theta$  and break the axial flavour symmetry. For the cases  $N_f = 1$  and  $N_f = 2$  all integrals can be performed analytically. While general theorems do not allow for a nonzero critical temperature, the model is found to exhibit a quasi-phase-structure: For finite  $L$  the condensate – seen as a function of  $\log(T)$  – stays almost constant up to a certain temperature (which depends on  $L$ ), where it shows a sharp crossover to a value which is exponentially close to zero. In the limit  $L \rightarrow \infty$  the known behaviour for the one-flavour Schwinger model is reproduced. In case of two flavours direct pictorial evidence is given that the theory undergoes a phase-transition at  $T_c = 0$ .

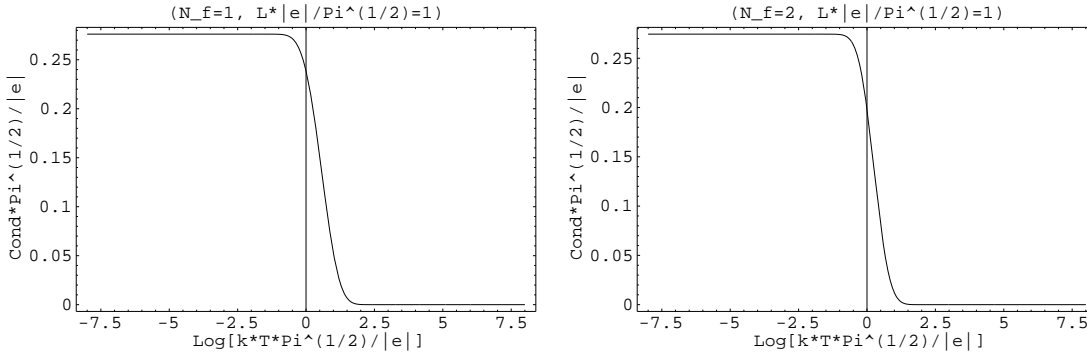


Figure 1: The (dimensionless) condensate  $|\langle\psi^\dagger P_\pm\psi\rangle|/\mu_1$  as a function of  $\log(kT/\mu_1)$  at fixed box-length  $L = 1/\mu_1$  (where  $\mu_1 = |e|/\pi^{1/2}$  is the induced single-flavour Schwinger mass (5)) for  $N_f = 1$  and  $N_f = 2$ .

## 1 Introduction

For realistic gauge field theories like QCD(4) it is in general an unsolved problem to determine their phase-structure (e.g. as a function of the fermion masses  $m_1 \dots m_{N_f}$ ) analytically. For this reason, one may either determine their phase-structure approximatively or try to attack the question in some simpler models analytically [1, 2].

For many questions arising in QCD, the Schwinger model [3] (QED in two dimensions with one or  $N_f$  massless fermions) has proven to be an interesting testing ground: It has shed some light on such longstanding problems of QCD as the  $U(1)_A$ -problem [4] and it has been used to test the validity of the Instanton Liquid Picture [5, 6].

However, for investigating symmetry-breakdown any two-dimensional model field theory doesn't seem to be of interest: There is no spontaneous breaking of a continuous global symmetry with associated Goldstone bosons in two dimensions [7] and a symmetry which is anomalously broken can't get restored at finite temperature [8].

It is the aim of the present paper to show that – in spite of the truth of this conventional wisdom – the Schwinger model exhibits an interesting quasi-phase-structure: The chiral condensate  $\langle\psi^\dagger \frac{1}{2}(1 \pm \gamma_5)\psi\rangle$  (which is used to probe the chiral symmetry) shows – as a function of the log of the temperature – a sharp crossover-behaviour: For any finite box-length  $L$  there is a well defined low-temperature regime where the condensate stays almost constant (the value depends on  $L$ ) and there is a “critical temperature” where the condensate decays (through a fairly well localized symmetry-quasi-restoration process) to a value which is exponentially close (but not equal) to zero.

Moreover, as the length  $L$  is sent to infinity, this behaviour is shown to imply that the two-flavour Schwinger model exhibits a phase-transition at  $T=0$  – which is a rederivation of a recent claim by Smilga and Verbaarschot [9]. A generalization to the case of  $N_f$  flavours is proposed.

The Schwinger model has had a great impact on the development of field theoretic ideas and techniques: The original quantization on the plane [10] suffered from the deficit that a direct calculation of the condensates  $\langle\psi^\dagger\psi\rangle$  and  $\langle\psi^\dagger\gamma_5\psi\rangle$  gave vanishing results whereas an indirect determination via the clustering theorem led to the standard nonzero value [11]. One decade ago the Schwinger model has been quantized on compact manifolds without

boundaries, the first ones being the (euclidean) sphere  $S^2$  [12] and the (euclidean) torus  $T^2$  [13]. In both cases direct calculations for the chiral condensates  $\langle \psi^\dagger \psi \rangle$  and  $\langle \psi^\dagger \gamma_5 \psi \rangle$  were found to yield nonvanishing results for finite volumes of the manifold.

Here we shall consider the model on a finite-temperature-cylinder with (anti-)periodic boundary conditions in the euclidean timelike direction, but with noncyclic boundary conditions in the spatial direction: On the two spatial ends (at  $x^1=0$  and  $x^1=L$ ) some chirality-breaking (XB-) boundary-conditions are imposed.

The motivation to use these XB-boundary-conditions stems again from QCD. There one would like to give a proof (without involving any assumption) that in the chiral limit the axial flavour symmetry  $SU(N_f)_A$  is spontaneously broken. The natural way to study a symmetry which is expected to be broken spontaneously is to break it explicitly and to try to determine how the system behaves in the limit when the external trigger is softly removed. For both QCD and the  $N_f$ -flavour Schwinger model this means that one has to break the axial  $N_f$ -flavour symmetry and then try to determine how some observables which are sensitive to its breaking do behave in the limit where the trigger term is removed. There is a long series of efforts in the literature which try to achieve this goal by studying either QCD or the  $N_f$ -flavour Schwinger model with a small fermion mass. In this approach the task is to determine how the chiral correlators behave in the limit where the fermion masses tend to be tiny as compared to the intrinsic mass of the theory. The problem with this particular method of breaking the axial flavour symmetry is that the value of the chiral condensate is related to the mean level density of the eigenvalues of the Dirac operator in the infrared [14], but the spectral density of the massive Dirac operator in a given gauge-field background is not (yet) known in general.

Together with A.Wipf, we have previously explored the alternative of breaking the chiral symmetry through introducing boundary conditions for the fermions rather than giving them a mass [15]. There we dealt with euclidean  $U(N_c)$  and  $SU(N_c)$  gauge-theories with  $N_f$  massless flavours quantized inside an even( $d=2n$ )-dimensional ball  $B_R^{2n}$  with boundary  $S_R^{2n-1}$  on which the XB-boundary-conditions considered in [16] have been imposed. These boundary conditions relate the different spin-components of each flavour on the boundary and are neutral with respect to vector-flavour-transformations. As a consequence the (gauge-invariant) fermionic determinant happens to be the same for all flavours. The most important result of this work was the observation that the XB-boundary-conditions proved to be equally suited to trigger a chiral condensate as are small fermion masses. From a technical point of view, the XB-boundary-conditions turned out to be very convenient: We succeeded in calculating the (massless) fermionic determinant in an arbitrary gauge-field background (the fields subject to the XB-boundary-conditions) and thus we were able to derive the analytical expressions for the chiral correlators (exploiting the rotational symmetry of  $B^2$ ).

In a second work [17], we examined whether the approach of breaking the  $SU(N_f)_A$ -symmetry by boundary-conditions can be extended to gauge-systems at finite temperature. Choosing the Schwinger model as a testbed the answer was in the affirmative: First of all we found that most of the nice features associated to the quantization on contractible manifolds (topologically equivalent to  $B^{2n}$ ) persist in the case of the finite temperature cylinder with XB-boundary-conditions at the spatial ends: The configuration space is still *topologically trivial* (i.e. without disconnected instanton sectors) and in particular there are *no fermionic zero-modes* (which usually tend to complicate the quantization considerably [13]). The technical difficulty we had to deal with is the fact that on non-contractible manifolds (e.g. a cylinder) the standard decomposition-technique for the Dirac operator, on which the quanti-

zation adopted in [15] heavily relied, could no longer be used. For this reason [17] turned out to be a rather technical paper, mostly devoted to show how this difficulty can be overcome.

The present paper concentrates on the physics which can be addressed from this setup. To be definite: The Schwinger model

$$S[A, \psi^\dagger, \psi] = S_B[A] + S_F[A, \psi^\dagger, \psi] \quad (1)$$

$$S_B = \frac{1}{4} \int_M F_{\mu\nu} F_{\mu\nu} \quad , \quad S_F = \sum_{n=1}^{N_f} \int_M \psi_n^\dagger i \not{D} \psi_n$$

in  $d = 2$  dimensions is studied on the manifold

$$M = [0, \beta] \times [0, L] \quad \ni \quad (x^0, x^1) \quad (2)$$

with volume  $V = \beta L$ . In euclidean time direction, the fields  $A$  and  $\psi$  are periodic and antiperiodic respectively with period  $\beta$ . Hence  $x^0 = 0$  and  $x^0 = \beta$  are identified (up to an eventual minus sign) and the manifold is a cylinder. At the spatial ends of the cylinder (at  $x^1 = 0$  and  $x^1 = L$ ) specific XB-boundary-conditions (to be discussed below) are imposed. Through explicit numerical evaluation of the analytical formulae we demonstrate that the model exhibits a quasi-phase-structure as described above. In particular we find that the two-flavour Schwinger model (limit  $L \rightarrow \infty$ ) exhibits a (true) phase-transition at  $T_c = 0$  – which is a rederivation of a result which was obtained by Smilga and Verbaarschot [9] using completely different technical tools.

For notational simplicity the following abbreviations are used

$$\tau = \frac{\beta}{2L} \quad , \quad \xi = \frac{x^1}{L} \quad (3)$$

as well as inverse temperature and box-length

$$\sigma \equiv \frac{|e|\beta}{\sqrt{\pi}} \quad , \quad \lambda \equiv \frac{|e|L}{\sqrt{\pi}} \quad (4)$$

rescaled by the Compton-wavelength associated to the single-flavour Schwinger mass and

$$\mu : \equiv \sqrt{\frac{N_f e^2}{\pi}} \quad (5)$$

which is the latter's generalization to the case of  $N_f$ -flavours.

This paper is organized as follows: In section 2 we briefly review the quantization of the model subject to the XB-boundary-conditions. In section 3 the analytical results for the chiral condensate  $\langle \psi^\dagger \frac{1}{2}(1 \pm \gamma_5) \psi \rangle(x)$  are re-expressed using theta-functions. In section 4 the remaining (c-number-)integrals within the analytic formulae for arbitrary  $N_f$  are fully performed for the cases  $N_f = 1$  and  $N_f = 2$ . This allows us to show explicit numerical evaluations of our analytical findings for these two cases revealing the two quasi-phases as described above and resulting in an explicit plot of the “quasi-phasestructure” (figure 7). In the concluding section 5 we try to illustrate our results and to relate them to the work by Smilga and Verbaarschot [9] and others.

## 2 Quantization with Thermal and XB-Boundary-Conditions

Here we shall give a short review of the conceptually relevant aspects of the quantization. For technical aspects the reader is referred to [17].

### 2.1 Chirality Breaking Boundary Conditions

The chirality-breaking (XB-)boundary-conditions as discussed in [16] can be motivated by the request that the Dirac operator  $i\mathcal{D}$  is symmetric under the scalar product  $(\chi, \psi) := \int \chi^\dagger \psi d^2x$ , which leads to the condition that the surface integral  $i \oint \chi^\dagger \gamma_n \psi ds$  vanishes, where  $\gamma_n = (\gamma, n) = n_\mu \gamma_\mu = \not{n}$  and  $n_\mu$  is the outward oriented normal vectorfield on the boundary. Imposing local linear boundary conditions which ensure this requirement amounts to have  $\chi^\dagger \gamma_n \psi = 0$  on the boundary for each pair. A sufficient condition is to have all modes obeying  $\psi = B\psi$  on the boundary, where the boundary operator  $B$  (which is understood to act as the identity in flavour space) is required to satisfy  $B^\dagger \gamma_n B = -\gamma_n$  and  $B^2 = 1$ . We shall choose the one-parameter family of boundary operators [16]

$$B \equiv B_\theta := i\gamma_5 e^{\theta\gamma_5} \gamma_n \quad (6)$$

which break the  $\gamma_5$  invariance of the theory, thus making the  $N_f$  flavour theory invariant under  $SU(N_f)_V$  instead of  $SU(N_f)_L \times SU(N_f)_R$ . They will be supplemented by suitable boundary conditions for the gauge-field. These boundary conditions prevent the  $U(1)$ -current from leaking through the boundary, since  $n \cdot j = \psi^\dagger \gamma_n \psi = 0$  on the boundary.

For explicit calculations we shall choose the chiral representation  $\gamma_0 = \sigma_1, \gamma_1 = \sigma_2$  and  $\gamma_5 = \sigma_3$  which implies that the explicit expressions for the boundary operators at the two ends of the cylinder (2) take the form

$$B_L = - \begin{pmatrix} 0 & e^\theta \\ e^{-\theta} & 0 \end{pmatrix} \text{ (at } x^1=0) \quad \text{and} \quad B_R = + \begin{pmatrix} 0 & e^\theta \\ e^{-\theta} & 0 \end{pmatrix} \text{ (at } x^1=L) \quad . \quad (7)$$

### 2.2 Immediate Consequences for the Spectrum

The decision to quantize with boundary condition  $\psi = B_\theta \psi$  with boundary operator (6) has direct consequences [15, 17, 18]:

- (i) The Dirac operator has a discrete real spectrum which is *asymmetric* w.r.t. zero.
- (ii) The spectrum is empty at zero, i.e. the Dirac operator has *no zero modes*.
- (iii) The instanton number  $q = \frac{e}{4\pi} \int \epsilon_{\mu\nu} F_{\mu\nu} = \frac{e}{2\pi} \int E \in \mathbf{R}$  is *not quantized*.

The first property already indicates that we are away from the usual Patodi-Singer-index-theorem situation. The second property implies that the generating functional for the fermions in a given gauge-field background  $A$

$$Z_F[A, \eta^\dagger, \eta] = \frac{1}{N_F} \int D\psi^\dagger D\psi e^{-\int \psi^\dagger i\mathcal{D}\psi + i \int \psi^\dagger \eta - i \int \eta^\dagger \psi} \quad (8)$$

is indeed given by the textbook formula

$$Z_F[A, \eta^\dagger, \eta] = \frac{\det_\theta(i\mathcal{D})}{\det_\theta(i\mathcal{D})} e^{\int \eta^\dagger (i\mathcal{D})^{-1} \eta} \quad (9)$$

and the chiral expectation values follow by taking the logarithmic derivative

$$\langle \psi^\dagger(x) P_\pm \psi(x) \rangle = \frac{1}{Z_F} \frac{\delta^2}{\delta \eta_\pm(x) \delta \eta_\pm^\dagger(x)} Z_F \Big|_{\eta_\pm = \eta_\pm^\dagger = 0} . \quad (10)$$

Throughout  $\theta$  is the free parameter in the boundary operator (7). The fact that the Feynman-Hellmann-boundary-formula  $\frac{d}{d\theta} \lambda_k = -\lambda_k(\psi_k, \gamma_5 \psi_k)$  [19] (where the  $\lambda_k$  denote the eigenvalues of  $i\mathcal{D}$ ) still holds true on the cylinder was the basis for the analytic determination of the  $\theta$ -dependence of the fermionic determinant  $\det_\theta(i\mathcal{D})$  performed in [17].

### 2.3 Neither Integer nor Fractional but Real Instanton Number

On a cylinder of finite spatial length the decomposition of a gauge potential  $A_\mu$  is [17]

$$\begin{aligned} eA_0 &= -\partial_1 \phi + \partial_0 \chi + \frac{2\pi}{\beta} c \\ eA_1 &= +\partial_0 \phi + \partial_1 \chi \end{aligned} \quad (11)$$

where  $\phi$  obeys Dirichlet boundary conditions at the ends ( $x^1 = 0, L$ ) and  $\chi$  is a pure gauge degree of freedom which fulfills  $\chi(0) + \chi(L) = 0$  and  $c \in [-1/2, 1/2[$  is the constant harmonic part. Thus the Dirac operator  $i\mathcal{D} = i\gamma_\mu(\partial_\mu - ieA_\mu)$  may be factorized

$$i\mathcal{D} = G^\dagger i\mathcal{D}_0 G \quad (12)$$

where  $i\mathcal{D}_0 = \gamma^0(i\partial_0 + 2\pi c/\beta) + \gamma^1 i\partial_1$  is the Dirac operator with the scalar parts switched off and  $G = \text{diag}(g^{*-1}, g)$  contains the prepotential  $g := e^{-(\phi+i\chi)}$  which is an element of the complexified gauge-group  $U(1)^* = S^1 \times \mathbf{R}_+$ .

On the cylinder there is a one-to-one-correspondence between  $\phi$  and  $eF_{01}$  if  $\phi$  obeys Dirichlet boundary-conditions at the two ends. The general field  $\phi$  may be decomposed as

$$\phi = \sum_{m \geq 0} \sum_{n \geq 1} \phi_{mn}^+ \cos\left(\frac{2\pi m x^0}{\beta}\right) \sin\left(\frac{\pi n x^1}{L}\right) + \phi_{mn}^- \sin\left(\frac{2\pi m x^0}{\beta}\right) \sin\left(\frac{\pi n x^1}{L}\right) \quad (13)$$

with coefficients  $\phi_{mn}^\pm \in \mathbf{R}$  decaying rapidly enough to make the series converge. The instanton-number is given by

$$q = \frac{e}{2\pi} \int E \, d^2x = \frac{1}{2\pi} \int \Delta \phi \, d^2x = -\frac{\beta}{L} \sum_{n \geq 1} \frac{1 - (-1)^n}{2} n \phi_{0n}^+ \quad (14)$$

where the decomposition (11) and the expansion (13) have been used. Given the result (14) it is obvious that the instanton-number  $q$  may take any real number.

### 2.4 Fermionic Propagator w.r.t. Boundary Conditions

In order to calculate the condensates one needs the Green's function  $S_\theta$  of the Dirac operator  $i\mathcal{D}$  on the cylinder subject to the XB-boundary-conditions. In addition to the defining relation  $(i\mathcal{D} S_\theta)(x, y) = \delta(x - y)$  this Green's function obeys the boundary-conditions

$$S_\theta(x^0 + \beta, x^1, y) = -S_\theta(x, y) \quad (15)$$

$$(B_L S_\theta)(x^0, x^1 = 0, y) = S_\theta(x^0, x^1 = 0, y) \quad (16)$$

$$(B_R S_\theta)(x^0, x^1 = L, y) = S_\theta(x^0, x^1 = L, y) \quad (17)$$

with  $B_{L/R}$  defined in (7) plus the adjoint relations with respect to  $y$ . The dependence of the gauge-potential has not been made explicit, since from the factorization-property (12) for the Dirac-operator it follows at once that  $S_\theta$  is related to the Green's function  $\tilde{S}_\theta$  of  $i\mathcal{D}_0$  as

$$S_\theta(x, y) = G^{-1}(x)\tilde{S}_\theta(x, y)G^{\dagger -1}(y) . \quad (18)$$

Indeed, since the field  $\phi$  obeys Dirichlet boundary-conditions at the ends of the cylinder the deformation matrix  $G$  appearing in (12) is unitary there and the boundary-conditions (15-17) transform into the identical ones for

$$\tilde{S}_\theta(x, y) = \begin{pmatrix} \tilde{S}_{++} & \tilde{S}_{+-} \\ \tilde{S}_{-+} & \tilde{S}_{--} \end{pmatrix}$$

where the indices refer to chirality. This Green's function – which carries the full  $c$ -dependence of  $S_\theta(x, y)$  – has been determined analytically [17] to read

$$\tilde{S}_\theta(x, y) = \frac{i}{2\pi} \cdot \sum_{m, n \in \mathbb{Z} \times \mathbb{Z}} (-1)^{(m+n)} \cdot e^{2\pi ic((x^0-y^0)/\beta-n)} \cdot \begin{pmatrix} e^\theta/r_{nm} & -(1/s_{nm}) \\ -(1/\bar{s}_{nm}) & e^{-\theta}/\bar{r}_{nm} \end{pmatrix}, \quad (19)$$

where  $r_{nm} = (x^0-y^0) + i(x^1+y^1) - (n\beta + 2imL)$  and  $s_{nm} = (x^0-y^0) + i(x^1-y^1) - (n\beta + 2imL)$ . From (19) it follows that the  $++$  and  $--$  elements at coinciding points inside the cylinder take the forms

$$\begin{aligned} \tilde{S}_\theta(x, x)_{\pm\pm} &= \pm \frac{e^{\pm\theta}}{4L} \sum_{n \in \mathbb{Z}} (-1)^n \frac{e^{\pm 2\pi inc}}{\sin(\pi(\xi - in\tau))} \\ &= \pm \frac{e^{\pm\theta}}{4L} \sum_{n \in \mathbb{Z}} (-1)^n \frac{\cos(2\pi nc) \sin(\pi\xi) \text{ch}(\pi n\tau) - \sin(2\pi nc) \cos(\pi\xi) \text{sh}(\pi n\tau)}{\sin^2(\pi\xi) + \text{sh}^2(\pi n\tau)} \end{aligned} \quad (20)$$

$$\begin{aligned} \tilde{S}_\theta(x, x)_{\pm\pm} &= \pm \frac{e^{\pm\theta}}{2\beta} \sum_{m \in \mathbb{Z}} (-1)^m \frac{e^{-2\pi(m+\xi)c/\tau}}{\sinh(\pi(m+\xi)/\tau)} \\ &= \pm \frac{e^{\pm\theta}}{2\beta} \sum_{m \in \mathbb{Z}} (-1)^m \frac{\text{ch}(2\pi(m+\xi)c/\tau) - \text{sh}(2\pi(m+\xi)c/\tau)}{\text{sh}(\pi(m+\xi)/\tau)} \end{aligned} \quad (21)$$

both valid for  $c \in [-\frac{1}{2}, \frac{1}{2}]$ . The two forms (20, 21) are equivalent but enjoy good convergence properties in the two regimes  $\beta \gg L$  and  $\beta \ll L$  respectively. From (18) the chirality violating entries of the fermionic Green's function on the diagonal take the form

$$S_\theta(x; x)_{\pm\pm} = e^{\mp 2\phi(x)} \tilde{S}_\theta(x; x)_{\pm\pm} \quad (22)$$

where  $\tilde{S}_{\pm\pm}$  plugged in from (20, 21) depends only on the harmonic part  $c$  in the decomposition (11) of the gauge-potential.

## 2.5 Fermionic Determinant w.r.t. Boundary Conditions

The arduous step was the computation of the  $\theta$ -dependence of the fermionic-determinant [17]. The Dirac-operator and the boundary-conditions are both flavour-neutral. Thus the determinant is the same for all flavours and it is sufficient to calculate it for one flavour. For

the explicit calculations we used the gauge-invariant  $\zeta$ -function definition of the determinant [20, 21]

$$\log \det_{\theta}(i\mathcal{D}) := \frac{1}{2} \log \det_{\theta}(-\mathcal{D}^2) := -\frac{1}{2} \frac{d}{ds} \Big|_{s=0} \zeta_{\theta}(-\mathcal{D}^2, s) \quad (23)$$

and calculated the  $\theta$ -dependence of the  $\zeta$ -function by means of a boundary-Feynman-Hellmann-formula. Denoting  $\{\mu_k | k \in \mathbf{N}\}$  the (positive) eigenvalues of  $-\mathcal{D}^2$ , the corresponding  $\zeta$ -function is defined and rewritten as a Mellin-transform in the usual way

$$\zeta_{\theta}(s) := \zeta_{\theta}(-\mathcal{D}^2, s) := \sum_k \mu_k^{-s} = \frac{1}{\Gamma(s)} \int_0^{\infty} t^{s-1} \text{tr}_{\theta}(e^{-t(-\mathcal{D}^2)}) dt \quad (24)$$

for  $\text{Re}(s) > d/2 = 1$  and its analytic continuation to  $\text{Re}(s) \leq 1$ .

The general task was to compute the normalized determinant

$$\frac{\det_{\theta}(i\mathcal{D})}{\det_0(i\mathcal{D})} \equiv \frac{\det_{\theta}(i\mathcal{D}_{1,c})}{\det_0(i\mathcal{D}_{0,0})} \quad (25)$$

where the first suffix on the r.h.s. indicates whether the scalar part is switched on and the  $c$  refers to the harmonic part in the decomposition (11). Together with  $\theta$  we thus have three parameters to switch off and this leaves us with  $3! = 6$  possible choices how to compute the functional determinant (25) in terms of three factors where each involves one switching only. We explicitly followed two of the six choices and found them to agree.

Our first choice was to calculate the functional determinant according to

$$\frac{\det_{\theta}(i\mathcal{D}_{1,c})}{\det_0(i\mathcal{D}_{0,0})} \equiv \frac{\det_{\theta}(i\mathcal{D}_{1,c})}{\det_0(i\mathcal{D}_{1,c})} \cdot \frac{\det_0(i\mathcal{D}_{1,c})}{\det_0(i\mathcal{D}_{0,c})} \cdot \frac{\det_0(i\mathcal{D}_{0,c})}{\det_0(i\mathcal{D}_{0,0})} \quad (26)$$

where we got for the first factor the explicit expression

$$\frac{\det_{\theta}(i\mathcal{D}_{1,c})}{\det_0(i\mathcal{D}_{1,c})} = \exp\left\{-\frac{\theta}{4\pi} \int e\epsilon_{\mu\nu} F_{\mu\nu}\right\} = \exp\left\{-\frac{\theta}{2\pi} \int \Delta\phi\right\}. \quad (27)$$

to be multiplied with the result

$$\frac{\det_0(i\mathcal{D}_{1,c})}{\det_0(i\mathcal{D}_{0,c})} = \exp\left\{\frac{1}{2\pi} \int \phi\Delta\phi\right\} \quad (28)$$

for the second factor. It is worth noting that with the first choice the term linear in  $\theta$  in the effective action stems from a volume-term (i.e.  $a_1(\cdot)$ ) in the Seeley-DeWitt-expansion.

Our second choice was to calculate the functional determinant according to

$$\frac{\det_{\theta}(i\mathcal{D}_{1,c})}{\det_0(i\mathcal{D}_{0,0})} \equiv \frac{\det_{\theta}(i\mathcal{D}_{1,c})}{\det_{\theta}(i\mathcal{D}_{0,c})} \cdot \frac{\det_{\theta}(i\mathcal{D}_{0,c})}{\det_0(i\mathcal{D}_{0,c})} \cdot \frac{\det_0(i\mathcal{D}_{0,c})}{\det_0(i\mathcal{D}_{0,0})} \quad (29)$$

where we found for the first factor the explicit expression

$$\frac{\det_{\theta}(i\mathcal{D}_{1,c})}{\det_{\theta}(i\mathcal{D}_{0,c})} = \exp\left\{\frac{1}{2\pi} \int \phi\Delta\phi - \frac{\theta}{2\pi} \int \Delta\phi\right\} \quad (30)$$

to be multiplied with the result

$$\frac{\det_{\theta}(i\mathcal{D}_{0,c})}{\det_0(i\mathcal{D}_{0,c})} = \exp\{0\} = 1 \quad (31)$$

for the second factor. It is worth noting that with the second choice the term linear in  $\theta$  in the effective action stems from a boundary-term (i.e.  $b_1(\cdot)$ ) in the Seeley-DeWitt-expansion.

In summary, the scattering of the fermions off the boundary generates a CP-odd term linear in  $\theta$  in the effective action for the gauge-bosons which is a two-dimensional artificial analogue of the QCD- $\theta$ -term.

The remaining task (which is to calculate the common third factor in the factorizations (26) and (29) of the functional determinant) was addressed by rewriting its logarithm as

$$\log \frac{\det_0(i\mathcal{D}_{0,c})}{\det_0(i\mathcal{D}_{0,0})} = -\frac{1}{2} \int_0^c \frac{d}{ds} \Big|_{s=0} \frac{d}{d\tilde{c}} \zeta_0(-\mathcal{D}_{0,\tilde{c}}^2, s) d\tilde{c} \quad . \quad (32)$$

and constructing the  $s$ -derivative at  $s = 0$  of the  $\tilde{c}$ -derivative of  $\zeta_0(-\mathcal{D}_{0,\tilde{c}}^2, s)$  explicitly. For that aim we computed the heat-kernel of the operator

$$-\mathcal{D}_{0,\tilde{c}}^2 = -\left((\partial_0 - 2\pi i\tilde{c}/\beta)^2 + \partial_1^2\right) I_2$$

for  $\theta = 0$  on the half-cylinder (see appendix of [17]) and from this expression we were able to derive

$$\Gamma(c) \equiv -\log \frac{\det_0(i\mathcal{D}_{0,c})}{\det_0(i\mathcal{D}_{0,0})} = \frac{V}{\pi} \sum' (-1)^{m+n} \frac{\cos(2\pi n c) - 1}{(n\beta)^2 + (2mL)^2} \quad (33)$$

as the result for the negative of the logarithm of the last factor of (26) and (29). In (33) and in the following the prime in the sum denotes the omission of the contribution from  $m = n = 0$ . By performing either the sum over  $m$  or the sum over  $n$  in (33) one gets

$$\Gamma(c) = \sum_{n \geq 1} \frac{(-1)^n}{n} \frac{\cos(2n\pi c) - 1}{\text{sh}(n\pi\beta/2L)} \quad (34)$$

$$\Gamma(c) = \sum_{m \geq 1} \frac{(-1)^m}{m} \frac{\text{ch}(4m\pi c L/\beta) - 1}{\text{sh}(2m\pi L/\beta)} + \frac{2\pi L}{\beta} c^2 \quad (35)$$

both valid for  $c \in [-1/2, 1/2]$  and periodically continued otherwise. These two equivalent forms will be useful in the low- and high- temperature expansion of the condensates.

## 2.6 Effective Action

The final step is to combine the classical (euclidean) action of the photon field, rewritten in the variables (11)

$$S_B[\phi] \equiv \frac{1}{4} F_{\mu\nu} F_{\mu\nu} = \frac{1}{2e^2} \Delta\phi\Delta\phi \quad (36)$$

with the result for the functional determinant (25). Collecting the contributions (27, 28) or (30, 31) as well as (34) or (35) and adding the classical action (36) one ends up with the effective action (which, of course, does not contain the gauge degree of freedom  $\chi$ )

$$\Gamma \equiv \Gamma_{\theta, N_f}[c, \phi] \equiv N_f \cdot \Gamma(c) + \Gamma_{\theta, N_f}[\phi] \quad (37)$$

where  $\Gamma(c)$  has been given in (34, 35) and  $\Gamma_{\theta, N_f}[\phi]$  is

$$\Gamma_{\theta, N_f}[\phi] \equiv \frac{1}{2e^2} \left\{ \int \phi \Delta^2 \phi - \mu^2 \int \phi \Delta \phi + \mu^2 \cdot \theta \int \Delta \phi \right\} \quad (38)$$

where the fact that the functional determinant is the same for all flavours has been used. In (38)  $\mu$  is the Schwinger mass (5) which is the analog of the  $\eta'$ -mass in 3-flavour-QCD.

In summary, the functional measure takes the form

$$d\mu_\theta[A] = \frac{1}{Z_\theta} e^{-\Gamma_{\theta, N_f}[c, \phi]} dc D\phi \delta(\chi) D\chi \quad (39)$$

where we have taken into account that the gauge-variation of the Lorentz gauge-condition  $F := \partial_\mu A^\mu = \Delta\chi$  and the Jacobian of the transformation from  $\{A\}$  to the variables  $\{\phi, c, \chi\}$  are independent of the fields. Actually, the corresponding determinants cancel each other.

We conclude that the expectation-value of any gauge-invariant operator  $O$  (which will not depend on  $\chi$ ) is given by

$$\langle O \rangle = \frac{\int dc D\phi O e^{-\Gamma_{\theta, N_f}[c, \phi]}}{\int dc D\phi e^{-\Gamma_{\theta, N_f}[c, \phi]}} \quad (40)$$

with  $\Gamma_{\theta, N_f}[c, \phi]$  given by (37, 38) and (34, 35).

### 3 Condensates in a Finite Volume

The general result (40) may be applied to calculate the chiral condensates as

$$\langle \psi^\dagger(x) P_\pm \psi(x) \rangle = \frac{\int dc D\phi S_\theta(x, x)_{\pm\pm} e^{-\Gamma_{\theta, N_f}[c, \phi]}}{\int dc D\phi e^{-\Gamma_{\theta, N_f}[c, \phi]}} \quad (41)$$

with  $S_\theta$  from (22) and  $\Gamma_\theta$  from (37). Both the (exponentiated) action and the Green's function factorize into parts which only depend on  $c$  and on  $\phi$ , respectively. Thus (41) factorizes as

$$\langle \psi^\dagger(x) P_\pm \psi(x) \rangle = C^\pm(x) \cdot D^\pm(x) \quad (42)$$

with  $x^0$ -independent factors

$$C^\pm(x^1) = \frac{\int dc \tilde{S}_\theta(x, x)_{\pm\pm} e^{-N_f \Gamma(c)}}{\int dc e^{-N_f \Gamma(c)}} \quad , \quad (43)$$

$$D^\pm(x^1) = \frac{\int D\phi e^{\mp 2\phi(x) - \Gamma_{\theta, N_f}[\phi]}}{\int D\phi e^{-\Gamma_{\theta, N_f}[\phi]}} \quad (44)$$

which depend on the parameters  $\theta, N_f, \beta, L$ . Here and below the  $c$ -integrals extend over the period  $[-1/2, 1/2]$ , whereas the field  $\phi$  is subject to Dirichlet boundary conditions at the two ends  $x^1 = 0$  and  $x^1 = L$ . The next step is to evaluate the factors  $C^\pm$  and  $D^\pm$  in (42) for a given circumference  $\beta$  and length  $L$  of the cylinder and given values of  $\theta$  and  $N_f$ .

#### 3.1 Harmonic Integral

In order to evaluate the first factor in (42) it is worth noticing that by using the two forms (34, 35) the factor  $\exp\{-\Gamma(c)\}$  can be rewritten in the two versions

$$e^{-\Gamma(c)} = \frac{\theta_3(c, i\tau)}{\theta_3(0, i\tau)} \quad (45)$$

$$e^{-\Gamma(c)} = e^{-\pi c^2/\tau} \frac{\theta_3(ic/\tau, i/\tau)}{\theta_3(0, i/\tau)} \quad (46)$$

respectively, which should be equivalent. Here we employed the notation

$$\theta_3(u, \omega) = \sum_{n \in \mathbb{Z}} e^{2\pi i n u} q^{n^2} = 1 + 2 \sum_{n \geq 1} \cos(2n\pi u) q^{n^2} \quad (q \equiv e^{i\pi\omega}) \quad (47)$$

for the parameters  $\omega = i\tau$  and  $\omega = i/\tau$  (giving real nome  $q \in ]0, 1[$ ) respectively. In deriving (45) and (46) we used the infinite-product expansion [22]

$$\theta_3(u, \omega) = \prod_{n \geq 1} (1 - q^{2n})(1 + 2q^{2n-1} \cos(2\pi u) + q^{2(2n-1)}) \quad (48)$$

and the addition theorem [23]

$$\ln \left( \frac{\theta_3(u+v, \omega)}{\theta_3(u-v, \omega)} \right) = 4 \sum_{n \geq 1} \frac{(-1)^n}{n} \frac{q^n}{1 - q^{2n}} \sin(2\pi n u) \sin(2\pi n v) \quad (49)$$

respectively. The Poisson resummation lemma makes sure that

$$\sum_{n \in \mathbb{Z}} e^{-(x+n)^2 \cdot t} = \sqrt{\pi/t} \sum_{n \in \mathbb{Z}} e^{-\pi^2 n^2/t} e^{2\pi i n x} \quad (x \in \mathbb{R}, t > 0) \quad (50)$$

from which we derive the theta-function duality relation

$$\sqrt{\tau} \theta_3(c, i\tau) = e^{-\pi c^2/\tau} \theta_3(\pm ic/\tau, i/\tau) \quad (c \in \mathbb{R}, \tau > 0) \quad (51)$$

which in turn allows to confirm the identity of the right-hand sides of (45) and (46).

Starting from expression (43) and plugging in the Green's function (20) as well as (45) or alternatively the Green's function (21) along with (46) one ends up with

$$C^\pm(x^1) = \pm \frac{e^{\pm\theta}}{4L} \sum_{n \in \mathbb{Z}} (-1)^n \frac{\sin(\pi\xi) \text{ch}(\pi n \tau)}{\sin^2(\pi\xi) + \text{sh}^2(\pi n \tau)} \cdot \frac{\int \cos(2\pi n c) \theta_3^{N_f}(c, i\tau) dc}{\int \theta_3^{N_f}(c, i\tau) dc} \quad (52)$$

$$C^\pm(x^1) = \pm \frac{e^{\pm\theta}}{2\beta} \sum_{m \in \mathbb{Z}} (-1)^m \frac{1}{\text{sh}(\pi(m+\xi)/\tau)} \cdot \frac{\int \text{ch}(2\pi(m+\xi)c/\tau) e^{-N_f \pi c^2/\tau} \theta_3^{N_f}(ic/\tau, i/\tau) dc}{\int e^{-N_f \pi c^2/\tau} \theta_3^{N_f}(ic/\tau, i/\tau) dc} \quad (53)$$

which is independent of  $x^0$  as required by translation-invariance. In the last step we have taken advantage from the fact that  $\theta_3(., .)$  is symmetric in its first argument and the  $c$ -integration is from  $-1/2$  to  $1/2$ .

### 3.2 Scalar Integral

For the evaluation of the second factor in (42) we recall that the integration extends over fields  $\phi$  which are periodic in the  $x^0$  and satisfy Dirichlet boundary-conditions at  $x^1 = 0, L$ . The first thing to do is to perform the gaussian integrals to get ( $\Delta'$  is the Laplacian taking derivatives w.r.t.  $x'$ )

$$D^\pm(x^1) = \exp \left\{ \frac{2\pi}{N_f} K(x, x) \right\} \cdot \exp \left\{ \pm \frac{\theta}{2} \cdot \int \Delta' K(x, x') d^2 x' \pm \frac{\theta}{2} \cdot \int \Delta' K(x', x) d^2 x' \right\} \quad (54)$$

where the integration is over  $x'$  and the kernel (employing the Schwinger mass (5))

$$K(x, y) = \langle x | \frac{\mu^2}{-\Delta(-\Delta + \mu^2)} | y \rangle = \langle x | \frac{1}{-\Delta} | y \rangle - \langle x | \frac{1}{-\Delta + \mu^2} | y \rangle \quad (55)$$

is with respect to Dirichlet boundary conditions. From its explicit form one finds [17]

$$K(x, x) = \frac{1}{2\pi} \sum_{n \geq 1} \left( 1 - \cos(2n\pi\xi) \right) \left( \frac{\text{cth}(n\pi\tau)}{n} - (n \rightarrow \sqrt{n^2 + (\mu L/\pi)^2}) \right) \quad (56)$$

$$K(x, x) = \frac{\xi(1-\xi)}{2\tau} + \frac{\text{ch}(\mu L(1-2\xi)) - \text{ch}(\mu L)}{2\mu\beta \text{sh}(\mu L)} + \frac{1}{2\pi} \sum_{m \geq 1} \frac{\text{ch}(m\pi/\tau) - \text{ch}(m\pi(1-2\xi)/\tau)}{m \text{sh}(m\pi/\tau)} - (m \rightarrow \sqrt{m^2 + (\mu\beta/2\pi)^2}) \quad (57)$$

which is perfectly finite as well as

$$\int \Delta' K(x, x') d^2 x' = \int \Delta' K(x', x) d^2 x' = \frac{\text{sh}(\mu L(1-\xi)) + \text{sh}(\mu L\xi)}{\text{sh}(\mu L)} - 1 \quad (58)$$

from which the factor (54) can be computed. As one can see, all three expressions (56, 57, 58) tend to zero as  $x$  approaches the boundary. The result for (54) is then found to read

$$D^\pm(x^1) = \exp \left\{ \frac{1}{N_f} \sum_{n \geq 1} \left( 1 - \cos(2n\pi\xi) \right) \left( \frac{\text{cth}(n\pi\tau)}{n} - (n \rightarrow \sqrt{n^2 + (\mu L/\pi)^2}) \right) \right\} \cdot \exp \left\{ \pm \theta \cdot \left( \frac{\text{sh}(\mu L(1-\xi)) + \text{sh}(\mu L\xi)}{\text{sh}(\mu L)} - 1 \right) \right\} \quad (59)$$

$$D^\pm(x^1) = \exp \left\{ \frac{2\pi}{N_f} \left( \frac{\xi(1-\xi)}{2\tau} + \frac{\text{ch}(\mu L(1-2\xi)) - \text{ch}(\mu L)}{2\mu\beta \text{sh}(\mu L)} \right) \right\} \cdot \exp \left\{ \frac{1}{N_f} \sum_{m \geq 1} \frac{\text{ch}(m\pi/\tau) - \text{ch}(m\pi(1-2\xi)/\tau)}{m \text{sh}(m\pi/\tau)} - (m \rightarrow \sqrt{m^2 + (\mu\beta/2\pi)^2}) \right\} \cdot \exp \left\{ \pm \theta \cdot \left( \frac{\text{sh}(\mu L(1-\xi)) + \text{sh}(\mu L\xi)}{\text{sh}(\mu L)} - 1 \right) \right\} \quad (60)$$

which is independent of  $x^0$  as required by translation-invariance.

### 3.3 Analytical Expression for Condensate at Arbitrary Points

The chiral condensate (42) is simply the product of (52) and (59) or equivalently (53) and (60). Rescaled by natural units (4), it takes the form

$$\frac{\langle \psi^\dagger P_\pm \psi \rangle(x^1)}{(|e|/\sqrt{\pi})} = \pm \frac{e^{\pm\theta \cdot \text{ch}(\lambda\sqrt{N_f}(1-2\xi)/2)/\text{ch}(\lambda\sqrt{N_f}/2)}}{4\lambda} \cdot \sum_{n \in \mathbb{Z}} (-1)^n \frac{\sin(\pi\xi) \text{ch}(\pi n\tau)}{\sin^2(\pi\xi) + \text{sh}^2(\pi n\tau)} \cdot \frac{\int \cos(2\pi n c) \theta_3^{N_f}(c, i\tau) dc}{\int \theta_3^{N_f}(c, i\tau) dc} \cdot \exp \left\{ \frac{1}{N_f} \sum_{n \geq 1} \left( 1 - \cos(2n\pi\xi) \right) \left( \frac{\text{cth}(n\pi\tau)}{n} - (n \rightarrow \sqrt{n^2 + N_f(\lambda/\pi)^2}) \right) \right\} \quad (61)$$

$$\begin{aligned}
\frac{\langle \psi^\dagger P_\pm \psi \rangle(x^1)}{(|e|/\sqrt{\pi})} &= \pm \frac{e^{\pm\theta \cdot \text{ch}(\lambda\sqrt{N_f}(1-2\xi)/2)/\text{ch}(\lambda\sqrt{N_f}/2)}}{2\sigma} \cdot \\
&\sum_{m \in \mathbb{Z}} (-1)^m \frac{1}{\text{sh}(\pi(m+\xi)/\tau)} \cdot \frac{\int \text{ch}(2\pi(m+\xi)c/\tau) e^{-N_f \pi c^2/\tau} \theta_3^{N_f}(ic/\tau, i/\tau) dc}{\int e^{-N_f \pi c^2/\tau} \theta_3^{N_f}(ic/\tau, i/\tau) dc} \cdot \\
&\exp \left\{ \frac{\pi}{N_f} \left( \frac{\xi(1-\xi)}{\tau} + \frac{\text{ch}(\lambda\sqrt{N_f}(1-2\xi)) - \text{ch}(\lambda\sqrt{N_f})}{\sigma\sqrt{N_f} \text{sh}(\lambda\sqrt{N_f})} \right) \right\} \cdot \quad (62) \\
&\exp \left\{ \frac{1}{N_f} \sum_{m \geq 1} \frac{\text{ch}(m\pi/\tau) - \text{ch}(m\pi(1-2\xi)/\tau)}{m \text{sh}(m\pi/\tau)} - (m \rightarrow \sqrt{m^2 + N_f(\sigma/2\pi)^2}) \right\}
\end{aligned}$$

where the  $\xi$ -independent but  $\theta$ -dependent parts of the two factors have cancelled. Note that the two forms (61) and (62) are identical for any finite (dimensionless) lengths  $\sigma$  and  $\lambda$ , but enjoy excellent convergence properties in the low- ( $\tau \gg 1$ ) and high- ( $\tau \ll 1$ ) temperature regimes, respectively.

## 4 Numerical Evaluation for $N_f = 1$ and $N_f = 2$

The general result (61, 62) shall be specialized to the cases  $N_f = 1$  and  $N_f = 2$  as the integration over  $c$  can be done in these cases. The aim is to collect specific observations concerning the difference between the single-flavour and multi-flavour case.

### 4.1 Specialization to $N_f = 1$ at Arbitrary Points

For the one-flavour-case the  $c$ -integrals in (61, 62) can be performed. Taking into account the fact that they extend over the interval  $[-1/2, 1/2]$  the result is found to read

$$\begin{aligned}
\frac{\langle \psi^\dagger P_\pm \psi \rangle}{(|e|/\sqrt{\pi})} &= \pm \frac{e^{\pm\theta \cdot \text{ch}(\lambda/2 - \lambda\xi)/\text{ch}(\lambda/2)}}{4\lambda} \sum_{n \in \mathbb{Z}} (-1)^n \frac{\sin(\pi\xi) \text{ch}(\pi n \tau)}{\sin^2(\pi\xi) + \text{sh}^2(\pi n \tau)} \exp(-n^2 \pi \tau) \cdot \\
&\exp \left\{ \sum_{n \geq 1} \left( 1 - \cos(2n\pi\xi) \right) \left( \frac{\text{cth}(n\pi\tau)}{n} - (n \rightarrow \sqrt{n^2 + (\lambda/\pi)^2}) \right) \right\} \quad (63)
\end{aligned}$$

$$\begin{aligned}
\frac{\langle \psi^\dagger P_\pm \psi \rangle}{(|e|/\sqrt{\pi})} &= \pm \frac{e^{\pm\theta \cdot \text{ch}(\lambda/2 - \lambda\xi)/\text{ch}(\lambda/2)}}{2\sigma} \sum_{m \in \mathbb{Z}} (-1)^m \frac{1}{\text{sh}(\pi(m+\xi)/\tau)} \times \\
&\frac{\sum_{k \in \mathbb{Z}} e^{\pi(m+\xi)(2k+m+\xi)/\tau} (\text{erf}(\frac{(k+m+\xi+1/2)\sqrt{\pi}}{\sqrt{\tau}}) - \text{erf}(\frac{(k+m+\xi-1/2)\sqrt{\pi}}{\sqrt{\tau}}))}{2} \cdot \\
&\exp \left\{ \pi \left( \frac{\xi(1-\xi)}{\tau} + \frac{\text{ch}(\lambda(1-2\xi)) - \text{ch}(\lambda)}{\sigma \text{sh}(\lambda)} \right) \right\} \cdot \\
&\exp \left\{ \sum_{m \geq 1} \frac{\text{ch}(m\pi/\tau) - \text{ch}(m\pi(1-2\xi)/\tau)}{m \text{sh}(m\pi/\tau)} - (m \rightarrow \sqrt{m^2 + (\sigma/2\pi)^2}) \right\} \quad (64)
\end{aligned}$$

where again the two equivalent representations (63) and (64) enjoy excellent convergence properties in the low- ( $\tau \gg 1$ ) and high- ( $\tau \ll 1$ ) temperature regimes, respectively.

## 4.2 Specialization to $N_f = 2$ at Arbitrary Points

For the two-flavour-case the  $c$ -integrals in (61, 62) can be performed. Taking into account the fact that they extend over the interval  $[-1/2, 1/2]$  the result is found to read

$$\frac{\langle \psi^\dagger P_\pm \psi \rangle}{(|e|/\sqrt{\pi})} = \pm \frac{e^{\pm\theta \cdot \text{ch}(\lambda/\sqrt{2} - \sqrt{2}\lambda\xi)/\text{ch}(\lambda/\sqrt{2})}}{4\lambda} \sum_{n \in \mathbb{Z}} (-1)^n \frac{\sin(\pi\xi) \text{ch}(\pi n\tau)}{\sin^2(\pi\xi) + \text{sh}^2(\pi n\tau)} \frac{\sum_{k \in \mathbb{Z}} e^{-(k^2 + (n-k)^2)\pi\tau}}{\sum_{k \in \mathbb{Z}} e^{-2k^2\pi\tau}} \cdot \exp \left\{ \frac{1}{2} \sum_{n \geq 1} (1 - \cos(2n\pi\xi)) \left( \frac{\text{cth}(n\pi\tau)}{n} - (n \rightarrow \sqrt{n^2 + 2(\lambda/\pi)^2}) \right) \right\} \quad (65)$$

$$\frac{\langle \psi^\dagger P_\pm \psi \rangle}{(|e|/\sqrt{\pi})} = \pm \frac{e^{\pm\theta \cdot \text{ch}(\lambda/\sqrt{2} - \sqrt{2}\lambda\xi)/\text{ch}(\lambda/\sqrt{2})}}{2\sigma} \sum_{m \in \mathbb{Z}} (-1)^m \frac{1}{\text{sh}(\pi(m + \xi)/\tau)} \times \frac{\sum_{q \in \mathbb{Z}} \sum_{p \in \mathbb{Z}} \frac{1 + (-1)^{p+q}}{2} e^{\pi((p+m+\xi)^2 - p^2 - q^2)/2\tau} (\text{erf}(\frac{(p+m+\xi+1)\sqrt{\pi}}{\sqrt{2\tau}}) - \text{erf}(\frac{(p+m+\xi-1)\sqrt{\pi}}{\sqrt{2\tau}}))}{2 \sum_{q \in \mathbb{Z}} e^{-\pi q^2/2\tau}} \cdot \exp \left\{ \frac{\pi}{2} \left( \frac{\xi(1-\xi)}{\tau} + \frac{\text{ch}(\sqrt{2}\lambda(1-2\xi)) - \text{ch}(\sqrt{2}\lambda)}{\sqrt{2}\sigma \text{sh}(\sqrt{2}\lambda)} \right) \right\} \cdot \exp \left\{ \frac{1}{2} \sum_{m \geq 1} \frac{\text{ch}(m\pi/\tau) - \text{ch}(m\pi(1-2\xi)/\tau)}{m \text{sh}(m\pi/\tau)} - (m \rightarrow \sqrt{m^2 + 2(\sigma/2\pi)^2}) \right\} \quad (66)$$

where again the two equivalent representations (65) and (66) enjoy excellent convergence properties in the low- ( $\tau \gg 1$ ) and high- ( $\tau \ll 1$ ) temperature regimes, respectively.

## 4.3 Numerical Evaluation of $\xi$ -Dependence

We are now in a position for evaluating formulas (63,64) for  $N_f = 1$  as well as formulas (65,66) for  $N_f = 2$ . The first hint regarding the difference between single-flavour and multi-flavour cases might come from observing how the spatial dependence of the condensate behaves as temperature and box-length vary. Since the condensate diverges on the boundaries as  $\xi^{-1}$  and  $(1 - \xi)^{-1}$  respectively <sup>1</sup>, it is the quantity  $4\xi(1 - \xi)|\langle \psi^\dagger P_\pm \psi \rangle|/(|e|/\sqrt{\pi})$  at  $\theta = 0$  which is displayed in figures 2 and 3.

By inspecting figures 2 and 3 one is lead to the observation that for any finite temperature the condensate ends up “creeping into the boundaries” (and fading away at any internal point of the box) once the box-length is sufficiently large.

On the other hand, cooling the system seems to have the opposite effect, i.e. to a first approximation, the shape of the spatial distribution of the condensate seems to depend on the ratio  $\tau = \sigma/2\lambda$ . However, as  $\sigma$  and  $\lambda$  both tend to be large, the spatial distribution starts to look qualitatively different in the two cases  $N_f = 1$  and  $N_f = 2$ , respectively. This is a pictorial hint indicating a difference between the single-flavour and the multi-flavour versions of the model once the twofold limit  $\sigma \rightarrow \infty, \lambda \rightarrow \infty$  is performed.

<sup>1</sup>There is no reason to start worrying: On the boundary the field has to satisfy a boundary condition which lets the free Green’s function take the form given in (19). This expression stays finite as one of its two entries –  $x$  or  $y$  – reaches the boundary but not if  $x$  and  $y$  reach the same point on the boundary, which means that there is no consistent double-boundary solution.

Figure 2: Spatial Dependence of  $4\xi(1-\xi)|\langle\psi^\dagger P_\pm\psi\rangle|\pi^{1/2}/|e|$  for  $N_f = 1$  ( $\xi = x^1/L$ ).

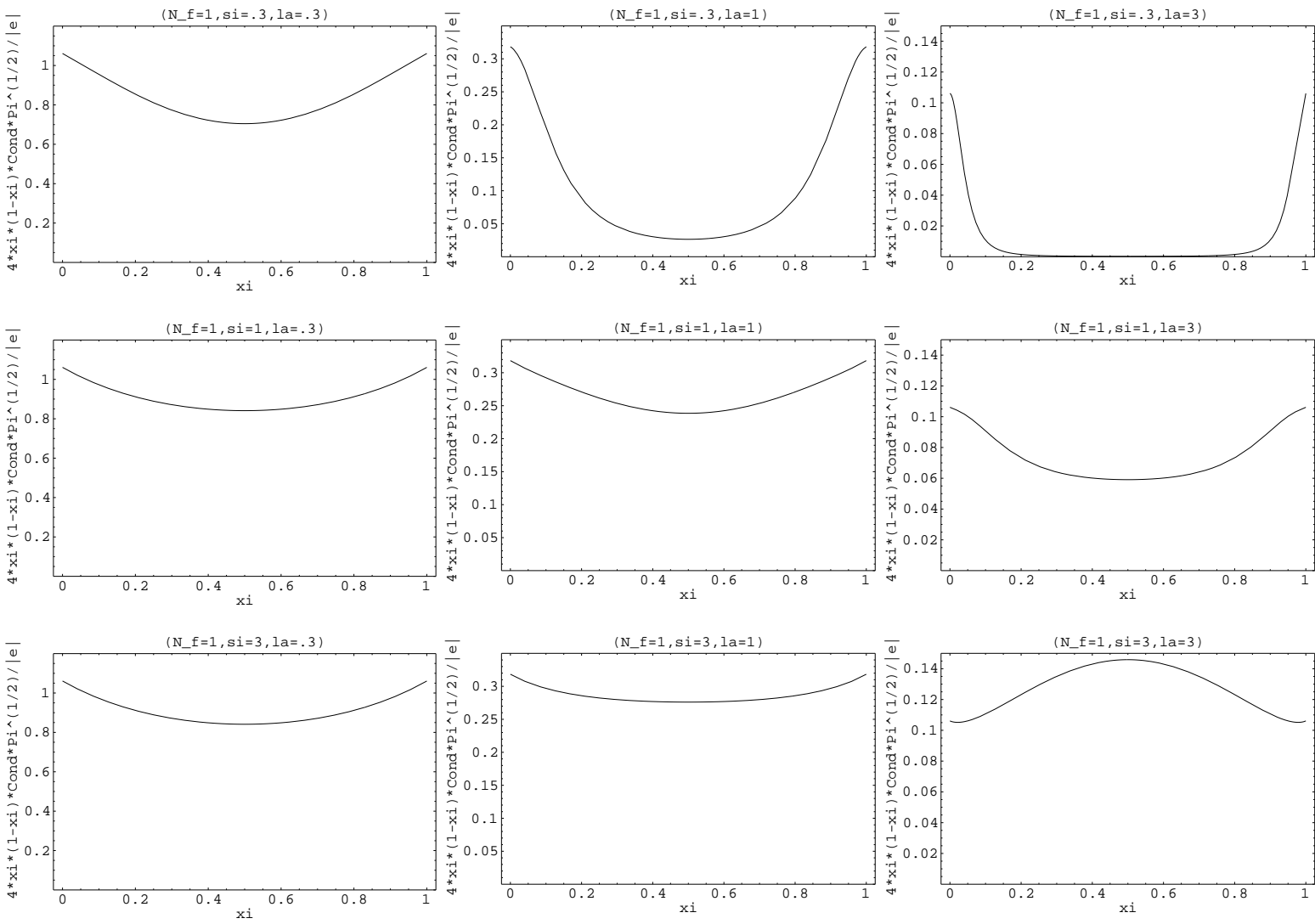
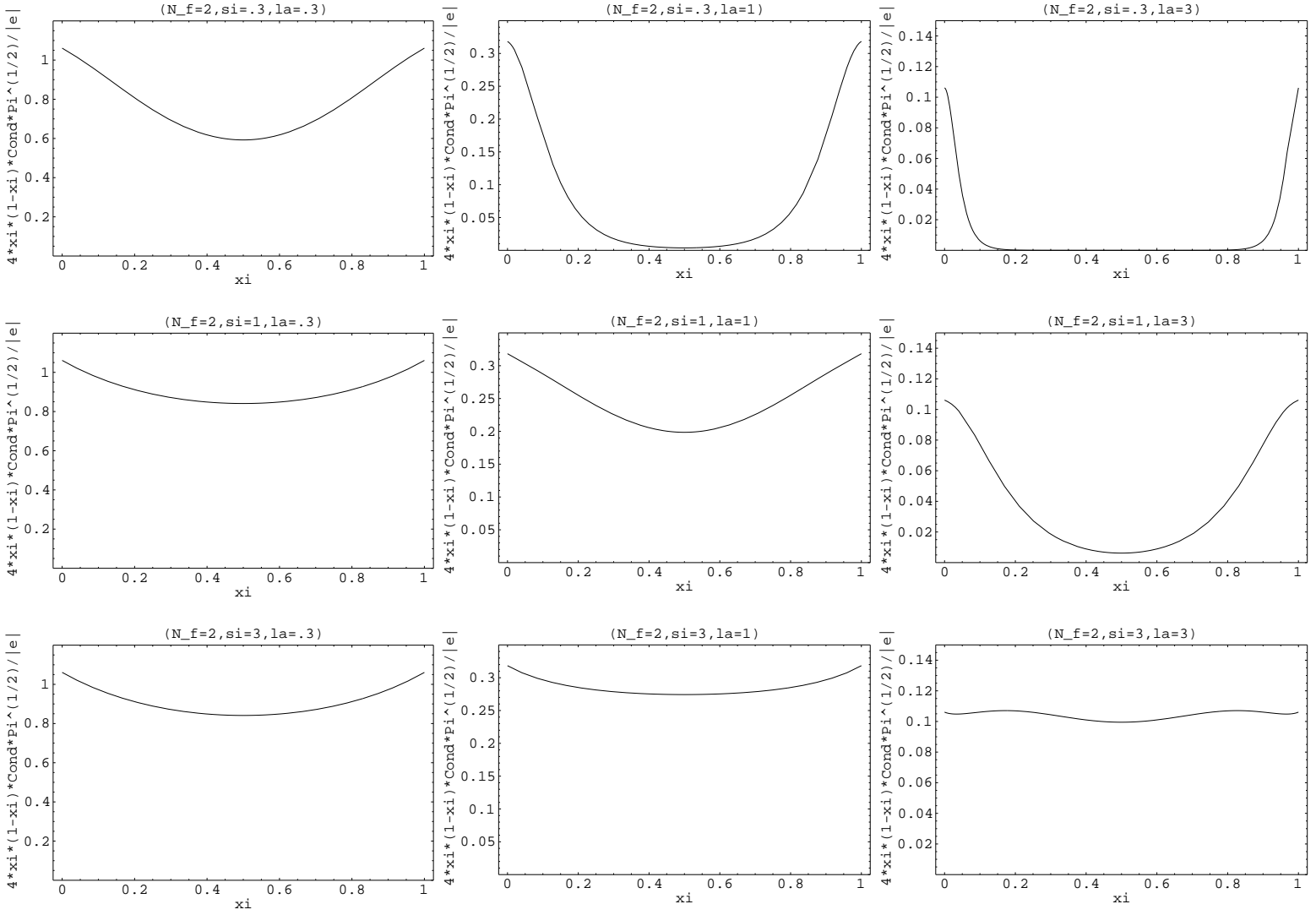


Figure 3: Spatial Dependence of  $4\xi(1-\xi)|\langle\psi^\dagger P_\pm\psi\rangle|\pi^{1/2}/|e|$  for  $N_f = 2$  ( $\xi = x^1/L$ ).



#### 4.4 Specialization to $N_f = 1$ at Midpoints

As one concentrates on the midpoints ( $\xi = 1/2$ ), formulae (63) and (64) take the form

$$\begin{aligned} \frac{\langle \psi^\dagger P_\pm \psi \rangle}{(|e|/\sqrt{\pi})} &= \pm \frac{e^{\pm\theta/\text{ch}(\lambda/2)}}{4\pi} \left( 1 + 2 \sum_{n \geq 1} (-1)^n \frac{1}{\text{ch}(n\pi\tau)} \exp(-n^2\pi\tau) \right) \cdot \\ &\quad \exp \left\{ \gamma - 2 \sum_{j \geq 1} (-1)^j K_0(j\lambda) \right\} \\ &\quad \exp \left\{ 4 \sum_{n \geq 0} \frac{1}{(2n+1)(e^{2(2n+1)\pi\tau} - 1)} - ((2n+1) \rightarrow \sqrt{(2n+1)^2 + (\lambda/\pi)^2}) \right\} \end{aligned} \quad (67)$$

$$\begin{aligned} \frac{\langle \psi^\dagger P_\pm \psi \rangle}{(|e|/\sqrt{\pi})} &= \pm \frac{e^{\pm\theta/\text{ch}(\lambda/2)}}{4\pi} \sum_{m \geq 0} (-1)^m \frac{e^{-\pi((2m+1)^2-1)/4\tau}}{\text{sh}(\pi(2m+1)/2\tau)} \times \\ &\quad \sum_{k \geq 0} \text{ch}\left(\frac{\pi(2m+1)(2k+1)}{2\tau}\right) \left( \text{erf}\left(\frac{(k+1)\sqrt{\pi}}{\sqrt{\tau}}\right) - \text{erf}\left(\frac{k\sqrt{\pi}}{\sqrt{\tau}}\right) \right) \cdot \\ &\quad \exp \left\{ \gamma + \frac{\pi(1 - \text{th}(\lambda/2))}{\sigma} - 2 \sum_{j \geq 1} K_0(j\sigma) \right\} \cdot \\ &\quad \exp \left\{ -2 \sum_{m \geq 1} \frac{1}{m(e^{m\pi/\tau} + 1)} - (m \rightarrow \sqrt{m^2 + (\sigma/2\pi)^2}) \right\} \end{aligned} \quad (68)$$

respectively (for details, see appendix), from which we derive

$$\lim_{\sigma \rightarrow \infty} \frac{\langle \psi^\dagger P_\pm \psi \rangle(\frac{L}{2})}{(|e|/\sqrt{\pi})} = \pm \frac{e^{\pm\theta/\text{ch}(\lambda/2)}}{4\pi} \exp \left\{ \gamma - 2 \sum_{j \geq 1} (-1)^j K_0(j\lambda) \right\} \quad (69)$$

$$\lim_{\lambda \rightarrow \infty} \frac{\langle \psi^\dagger P_\pm \psi \rangle(\frac{L}{2})}{(|e|/\sqrt{\pi})} = \pm \frac{1}{4\pi} \exp \left\{ \gamma - 2 \sum_{j \geq 1} K_0(j\sigma) \right\} \quad (70)$$

for  $N_f = 1$ . Thus

$$\lim_{\lambda \rightarrow \infty} \lim_{\sigma \rightarrow \infty} \frac{\langle \psi^\dagger P_\pm \psi \rangle(\frac{L}{2})}{(|e|/\sqrt{\pi})} = \pm \frac{1}{4\pi} e^\gamma = \lim_{\sigma \rightarrow \infty} \lim_{\lambda \rightarrow \infty} \frac{\langle \psi^\dagger P_\pm \psi \rangle(\frac{L}{2})}{(|e|/\sqrt{\pi})} \quad (71)$$

for  $N_f = 1$ . Note that (70) and the second equality in (71) correct for an erroneous result in [17] which was won by performing the limit under the integral.

#### 4.5 Specialization to $N_f = 2$ at Midpoints

As one concentrates on the midpoints ( $\xi = 1/2$ ), formulae (65) and (66) take the form

$$\begin{aligned} \frac{\langle \psi^\dagger P_\pm \psi \rangle}{(|e|/\sqrt{\pi})} &= \pm \frac{2^{1/4} e^{\pm\theta/\text{ch}(\lambda/\sqrt{2})}}{4\sqrt{\pi} \sqrt{\lambda}} \cdot \\ &\quad \left( 1 + 2 \sum_{n \geq 1} (-1)^n \frac{e^{-n^2\pi\tau/2}}{\text{ch}(n\pi\tau)} \cdot \frac{e^{-n^2\pi\tau/2} + 2 \sum_{k \geq 1} \frac{e^{-(n/2-k)^2 2\pi\tau} + e^{-(n/2+k)^2 2\pi\tau}}{2}}{1 + 2 \sum_{k \geq 1} e^{-2k^2\pi\tau}} \right) \cdot \end{aligned}$$

$$\exp\left\{\frac{\gamma}{2} - \sum_{j \geq 1} (-1)^j K_0(j\sqrt{2}\lambda)\right\}$$

$$\exp\left\{2 \sum_{n \geq 0} \frac{1}{(2n+1)(e^{2(2n+1)\pi\tau} - 1)} - ((2n+1) \rightarrow \sqrt{(2n+1)^2 + 2(\lambda/\pi)^2})\right\} \quad (72)$$

$$\frac{\langle \psi^\dagger P_\pm \psi \rangle}{(|e|/\sqrt{\pi})} = \pm \frac{2^{1/4} e^{\pm\theta/\text{ch}(\lambda/\sqrt{2})}}{4\sqrt{\pi} \sqrt{\sigma}} \sum_{m \geq 0} (-1)^m \frac{e^{-\pi((2m+1)^2 - 1)/8\tau}}{\text{sh}(\pi(2m+1)/2\tau)} \times$$

$$\frac{\sum_{q \in Z} e^{-\pi q^2/2\tau} \sum_{p \geq 0} \text{ch}\left(\frac{\pi(p+1/2)(m+1/2)}{\tau}\right) (\text{erf}\left(\frac{p+3/2}{\sqrt{2\tau/\pi}}\right) - \text{erf}\left(\frac{p-1/2}{\sqrt{2\tau/\pi}}\right)) + \sum_{q \in Z} e^{-\pi q^2/2\tau} \sum_{p \geq 0} (-1)^{p+q-m} \text{sh}\left(\frac{\pi(p+1/2)(m+1/2)}{\tau}\right) (\text{erf}\left(\frac{p+3/2}{\sqrt{2\tau/\pi}}\right) - \text{erf}\left(\frac{p-1/2}{\sqrt{2\tau/\pi}}\right))}{\sum_{q \in Z} e^{-\pi q^2/2\tau}}$$

$$\exp\left\{\frac{\gamma}{2} + \frac{\pi(1 - \text{th}(\lambda/\sqrt{2}))}{2\sqrt{2}\sigma} - \sum_{j \geq 1} K_0(j\sqrt{2}\sigma)\right\}$$

$$\exp\left\{-\sum_{m \geq 1} \frac{1}{m(e^{\pi m/\tau} + 1)} - (m \rightarrow \sqrt{m^2 + 2(\sigma/2\pi)^2})\right\} \quad (73)$$

respectively (for details, see appendix), from which we derive

$$\lim_{\sigma \rightarrow \infty} \frac{\langle \psi^\dagger P_\pm \psi \rangle(\frac{L}{2})}{(|e|/\sqrt{\pi})} = \pm \frac{2^{1/4} e^{\pm\theta/\text{ch}(\lambda/\sqrt{2})}}{4\sqrt{\pi} \sqrt{\lambda}} \exp\left\{\frac{\gamma}{2} - \sum_{j \geq 1} (-1)^j K_0(j\sqrt{2}\lambda)\right\} \quad (74)$$

$$\lim_{\lambda \rightarrow \infty} \frac{\langle \psi^\dagger P_\pm \psi \rangle(\frac{L}{2})}{(|e|/\sqrt{\pi})} = 0 \quad (75)$$

for  $N_f = 2$ . Thus

$$\lim_{\lambda \rightarrow \infty} \lim_{\sigma \rightarrow \infty} \frac{\langle \psi^\dagger P_\pm \psi \rangle(\frac{L}{2})}{(|e|/\sqrt{\pi})} = 0 = \lim_{\sigma \rightarrow \infty} \lim_{\lambda \rightarrow \infty} \frac{\langle \psi^\dagger P_\pm \psi \rangle(\frac{L}{2})}{(|e|/\sqrt{\pi})} \quad (76)$$

for  $N_f = 2$ . Note that in the first case the condensate decays rather reluctantly ( $\propto 1/\sqrt{\lambda}$ ) only under the outer limit, whereas in the second case it decays exponentially fast under the inner limit already (see appendix). This difference may be stated in equations through

$$\lim_{\lambda \rightarrow \infty} \lim_{\sigma \rightarrow \infty} \sqrt{\lambda} \frac{\langle \psi^\dagger P_\pm \psi \rangle(\frac{L}{2})}{(|e|/\sqrt{\pi})} = \pm \frac{2^{1/4}}{4\sqrt{\pi}} \exp\left\{\frac{\gamma}{2}\right\} \quad (77)$$

$$\lim_{\sigma \rightarrow \infty} \lim_{\lambda \rightarrow \infty} \sqrt{\lambda} \frac{\langle \psi^\dagger P_\pm \psi \rangle(\frac{L}{2})}{(|e|/\sqrt{\pi})} = 0 \quad (78)$$

which is peculiar for  $N_f = 2$ .

## 4.6 Numerical Evaluation at Midpoints

We are now in a position for numerically evaluating formulas (67, 68) for  $N_f = 1$  as well as formulas (72, 73) for  $N_f = 2$ .

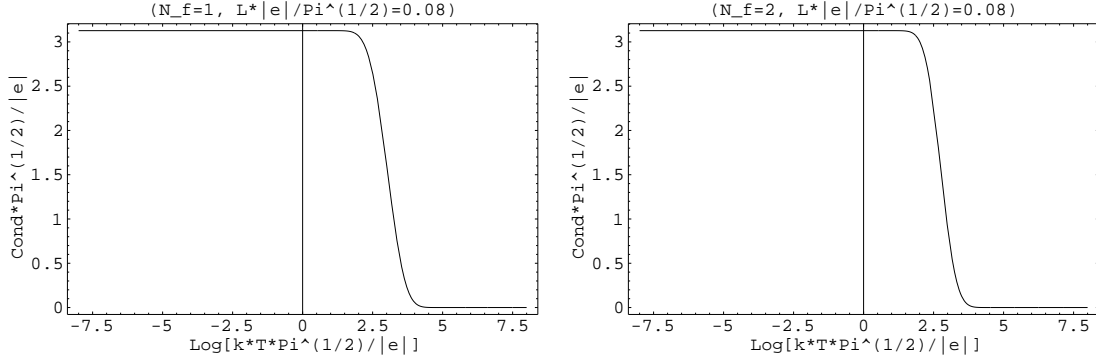


Figure 4:  $|\langle \psi^\dagger P_\pm \psi \rangle|/\mu_1$  as a function of  $\log(kT/\mu_1)$  at  $L = 0.08/\mu_1$  for  $N_f = 1$  and  $N_f = 2$ .

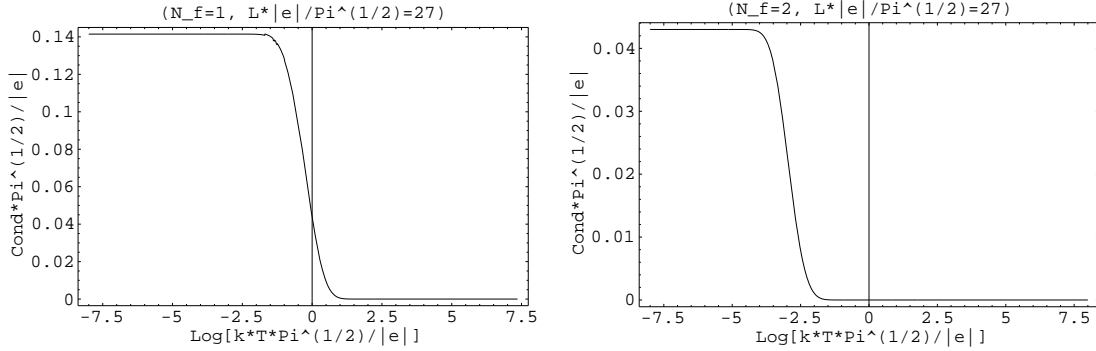


Figure 5:  $|\langle \psi^\dagger P_\pm \psi \rangle|/\mu_1$  as a function of  $\log(kT/\mu_1)$  at  $L = 27.0/\mu_1$  for  $N_f = 1$  and  $N_f = 2$ .

The following figures display the value of the condensate at  $\theta=0$  in the center of the box ( $\xi=1/2$ ). The two-dimensional graphs show the condensate as a function of  $\sigma = \beta \cdot |e|/\pi^{1/2}$  (or a function thereof) at fixed value of  $\lambda = L \cdot |e|/\pi^{1/2}$ . Throughout we use  $\mu_1 = |e|/\pi^{1/2}$ . The surface- and density-plots show the condensate versus (a function of)  $\sigma$  and  $\lambda$ .

It might be worth mentioning that in each of those figures both representations – (83) and (85) in case of  $N_f = 1$  as well (87) and (88) in case of  $N_f = 2$  – were used, the former formulas got evaluated for low temperatures ( $\tau \gg 1$ ), the latter ones got evaluated for high temperatures ( $\tau \ll 1$ ) — the switching being done in the region of the crossover transition, which essentially gives a numerical check that the representations (83) and (85) as well as the representations (87) and (88) indeed might be identical.

From figures 4 and 5 the system is seen to undergo a surprisingly well-localized crossover, which – however – doesn’t meet the criteria for a phase-transition of whatever kind as it is arbitrarily smooth (i.e.  $\in C^\infty$ ).

By comparing figures 4 and 5, one realizes that increasing the box-length essentially moves the “kink” to the left, i.e. increasing the box-length results in a decrease of the “critical temperature” (the effect being much stronger in case  $N_f=2$  than for  $N_f=1$ ) and one starts wondering whether this kink-phenomenon survives the limit  $L \rightarrow \infty$ . We will see that the answer to this question depends in a critical way on the number of flavours; the two cases  $N_f=1$  and  $N_f=2$  turn out to be different. The “plateaux” seem to be equally heigh for one

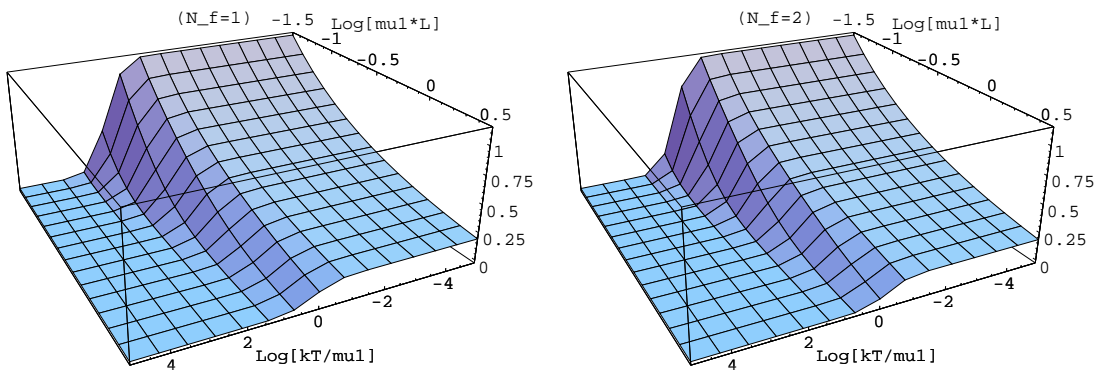


Figure 6:  $|\langle\psi^\dagger P_\pm\psi\rangle|/\mu_1$  as a function of  $\log(kT/\mu_1)$  and  $\log(L\mu_1)$  for  $N_f = 1$  and  $N_f = 2$ .

and two flavours as long as the box-length is small (figure 4) but the height of the plateau decays unequally rapidly if the box-length is increased (figure 5).

In order to reach an intuitive understanding it might be worth to have a look at figure 6. Thereby one realizes that there is a considerable fraction of the  $\log(kT/\mu_1)$ - $\log(L\mu_1)$ -plane where the condensate is exponentially close (but not equal) zero. Thus it might be helpful to introduce the concept of a *quasi-phase* with *almost* restored chiral symmetry. In order to do so one has to decide on a trigger-value which the condensate has to exceed in order to constitute a point (in the  $\log(kT/\mu_1)$ -  $\log(L\mu_1)$ -plane) with manifestly broken symmetry. While this choice is – in principle – arbitrary, it seems most reasonable to choose half of the classical value for the condensate in the classical (one-flavour) Schwinger model as the discriminator which makes the distinction between the two “quasi-phases”. Numerically, it is about 0.07.

Doing so results in generating the two contour-plots in figure 7: White points are those which satisfy the criterion  $|\langle\psi^\dagger P_\pm\psi\rangle| \geq e^\gamma \sqrt{e^2/\pi}/8\pi$  – they constitute the (quasi-)phase with *manifestly broken symmetry*. Black points are those which satisfy the criterion  $|\langle\psi^\dagger P_\pm\psi\rangle| \leq e^\gamma \sqrt{e^2/\pi}/8\pi$  – they constitute the quasi-phase with *quasi-restored symmetry*.

These two quasi-phases are separated by a “crossover-line” which lies to the r.h.s. of the point  $\beta = L = \infty$  (upper left corner) in case of  $N_f = 1$  but to the l.h.s. of this corner for  $N_f = 2$ . Thus the point  $\beta = L = \infty$  lies in the broken (quasi-)phase for  $N_f = 1$  and in the “unbroken” quasi-phase for  $N_f = 2$  – which hardly comes as a surprise. However, the concept of quasi-phases proves useful, as it tells us much more than this well-known result.

First of all we notice that the point  $\beta = L = 0$  (lower right corner in figure 7) lies right on the crossover-line in either case  $N_f = 1$  and  $N_f = 2$  (note that data close to the boundaries are cut off for numerical reasons). This observation lets us go back to formulas (61) and (62) and derive the (moderately interesting) noncommutativity-phenomenon

$$\lim_{L \rightarrow 0} \lim_{\beta \rightarrow 0} \langle\psi^\dagger P_\pm\psi\rangle\left(\frac{L}{2}\right) = 0 \quad (\forall N_f) \quad (79)$$

$$\lim_{\beta \rightarrow 0} \lim_{L \rightarrow 0} \langle\psi^\dagger P_\pm\psi\rangle\left(\frac{L}{2}\right) = \infty \quad (\forall N_f) \quad (80)$$

which is universal for any number of flavours.

The real virtue of the quasi-phase-structure-plot (figure 7) is that it shows that in the two-flavour case the point  $\beta = L = \infty$  – though being within the quasi-restored pseudophase –

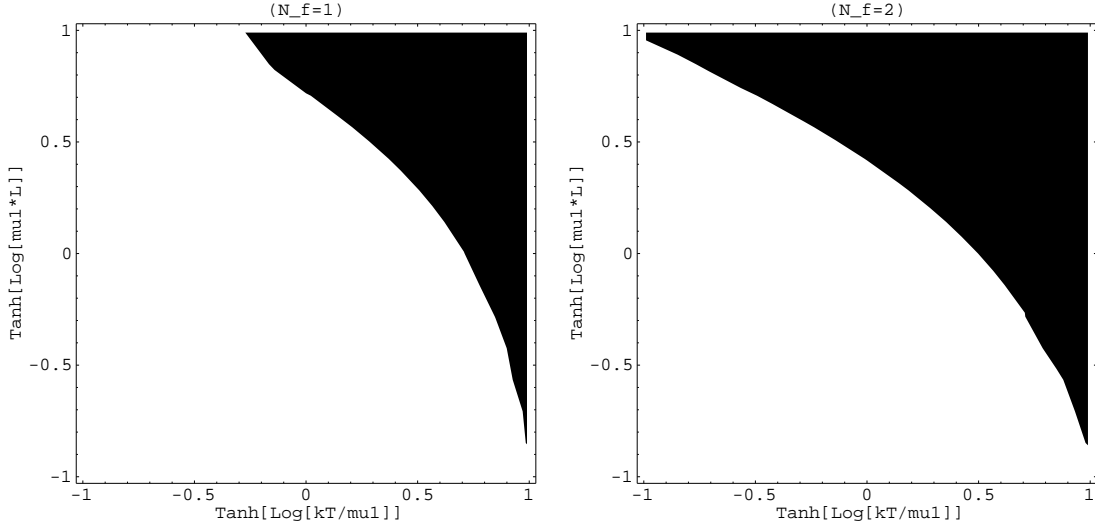


Figure 7: Quasi-Phasestructure as a function of  $\log(kT/\mu_1)$  and  $\log(L\mu_1)$  for  $N_f = 1$  and  $N_f = 2$ , respectively. Definition: see text.

actually lies very close to the crossover-line. An attempt to zoom into the upper left corner in these quasi-phasestructure plots results in figure 8.

From the l.h.s. of figure 8 we learn that the one-flavour-system approaches its standard-value for the conventional order-parameter in a very unspectacular way. However, the r.h.s. of figure 8 tells us that the two-flavour-system depends in the large- $L$ -limit in a very sensitive way on whether the temperature is zero or finite. This is exactly what we find from inspecting formulas (74, 75): At zero temperature the condensate goes to zero under  $\lambda \rightarrow \infty$  – but only very reluctantly:  $\propto 1/\sqrt{\lambda}$ . On the other hand, for any fixed finite temperature, the condensate vanishes exponentially fast under  $\lambda \rightarrow \infty$ .

If we consider the alternative order parameter  $2^{7/4}\pi^{1/2}e^{-\gamma} \cdot \sqrt{\lambda} |\langle \psi^\dagger P_\pm \psi \rangle|/\mu_1$  for  $N_f=2$  we end up saying that it acquires a finite value (which is exactly 1 in this normalization) at  $\beta = L = \infty$  if we take the zero-temperature-limit first and the limit of infinite box-length thereafter. On the other hand, if we perform  $L \rightarrow \infty$  before  $\beta \rightarrow \infty$  the novel order-parameter ends up being zero – as expressed in (77, 78) and confirmed by the r.h.s. of figure 9.

It is worth emphasizing that there is nothing wrong with the novel order-parameter  $2^{7/4}\pi^{1/2}e^{-\gamma} \cdot \sqrt{\lambda} |\langle \psi^\dagger P_\pm \psi \rangle|/\mu_1$  for  $N_f=2$  – in fact, the exponent 1/2 of the prefactor  $\lambda$  is *critical* in that sense that any other function of  $\lambda$  either makes the potential order-parameter blow up to infinity or meld down to zero as  $\lambda \rightarrow \infty$  is performed at zero temperature. Thus  $2^{7/4}\pi^{1/2}e^{-\gamma} \cdot \sqrt{\lambda} |\langle \psi^\dagger P_\pm \psi \rangle|/\mu_1$  is the unique choice for an order-parameter which exhibits the physics of the two-flavour system in the two-fold  $\beta, \lambda \rightarrow \infty$  limit.

The quasi-phasestructure-plot of the two-flavour system with this novel order-parameter would almost look like the r.h.s. of figure 7 – except that the crossover-line (the trigger-value being 0.5) now exactly goes through the upper left corner. Thus we would be led to the conclusion that in the  $N_f=2$  case the point  $\beta = L = \infty$  can be reached out of two different pseudo-phases – which also follows directly from inspecting the r.h.s. of figure 9.

In view of the result (77, 78) one might say that in the two-flavour system with the pseudo-phases defined through the novel order-parameter the corner  $\beta = L = \infty$  represents

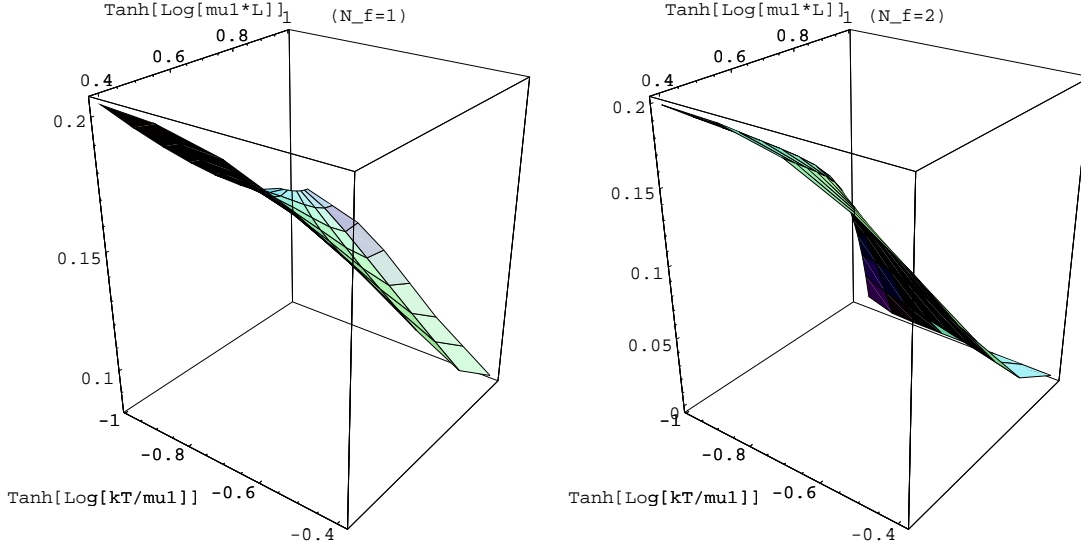


Figure 8: Zoom-out of the upper left corner of figure 7 for  $N_f = 1$  and  $N_f = 2$ .

a point where a (manifestly) broken and a (truly) restored phase (the prefix “pseudo” is unnecessary here) *coexist*. The crucial difference to the situation in the one-flavour system is that the (novel) order parameter at  $T > 0, L = \infty$  (corresponds to the upper border in figure 7) is *exactly zero* for  $N_f = 2$ . Moreover, from looking at figure 9 one realizes that the two limits (77, 78) represent nothing but the two extremes of how the relative weights may be set: In case of  $N_f = 2$  the order-parameter  $2^{7/4} \pi^{1/2} e^{-\gamma} \cdot \sqrt{\lambda} \langle \psi^\dagger P_\pm \psi \rangle / \mu_1$  can be given *any value* out of the interval  $[0, (\pm)1]$  by starting from an arbitrary point having the desired value and following the corresponding “line-of-constant-altitude” (in figure 9) towards  $\beta = L = \infty$ . On the other hand, for  $N_f = 1$  the same isn’t possible since  $\langle \psi^\dagger P_\pm \psi \rangle$  already has a finite value at  $\beta = L = \infty$ , i.e. the “critical” exponent for the prefactor  $\lambda$  is zero if  $N_f = 1$ . Our findings for the two-flavour-system may be formulated as follows: The absolute value of the (novel) order-parameter (which includes a prefactor  $\lambda^{1/2}$ ) is *single-valued* for any combination of strict-positive  $\beta$  and  $L$  – including either of them being infinite – except for the combination  $\beta = L = \infty$ . Through the corresponding “line-of-constant-altitude-approach” the relative weights of the two phases the two-flavour system at  $\beta = L = \infty$  is composed of may be precisely steered for.

Thus we establish the picture of  $\beta = L = \infty$  being a point where a (true) phase-transition occurs if  $N_f = 2$  but not for  $N_f = 1$  – as originally proposed by Smilga and Verbaarschot [9]. Regarding its classification we observe that the novel order-parameter (which may take any value out of the interval  $[0, (\pm)1]$ ) makes a finite jump when one re-enters the area  $\beta < \infty, L < \infty$  with any direction other than the one determined by the tangent (in the endpoint) to the corresponding “line-of-constant-altitude” (in figure 9). Thus it seems plausible to classify the transition as of first order (as far as such a classification may make sense when  $T_c = 0$ ). However, the r.h.s. of figure 9 also teaches us that for any finite box-length the (novel) order-parameter shows a well-localized but smooth crossover as a function of  $\beta$ . Taking this into account, it seems most reasonable to identify  $\beta = \lambda = \infty$  as a “critical point” for the two-flavour system.

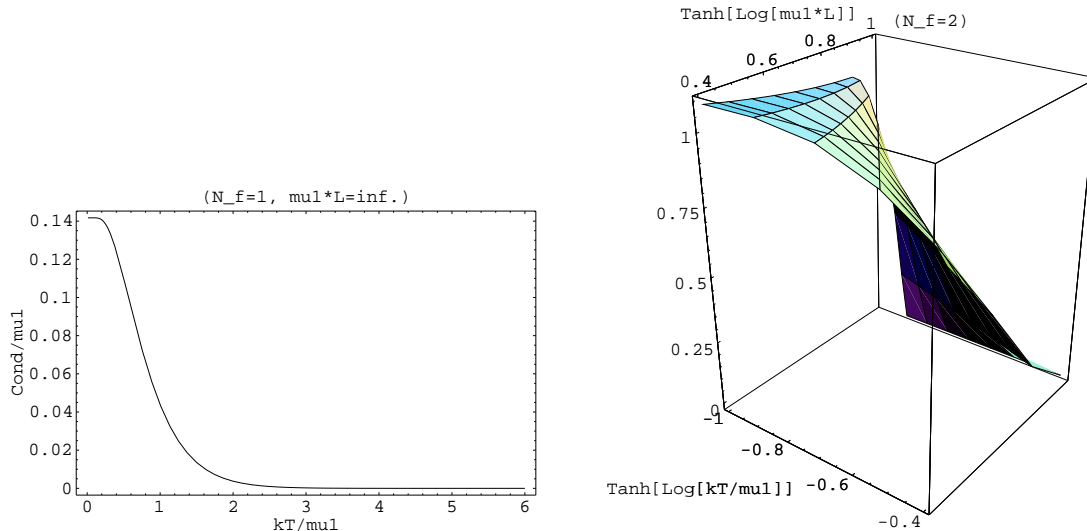


Figure 9: Left: One-flavour order-parameter  $|\langle\psi^\dagger P_\pm\psi\rangle|/\mu_1$  as a function of the dimensionless temperature at infinite box-length. Right: Zoom-out of the upper left corner in the analogue of figure 7 with the two-flavour order parameter  $2^{7/4}\pi^{1/2}e^{-\gamma}\cdot\lambda^{1/2}|\langle\psi^\dagger P_\pm\psi\rangle|/\mu_1$  rather than  $\langle\psi^\dagger P_\pm\psi\rangle/\mu_1$  – displaying the noncommutativity phenomenon (77, 78).

## 5 Discussion and Conclusion

The present paper has been devoted to a study of the  $N_f$ -flavour euclidean Schwinger model on a finite-temperature cylinder with  $SU(N_f)_A$  breaking local boundary conditions at the two spatial ends. We have investigated the value of the dimensionless condensate  $\langle\psi^\dagger P_\pm\psi\rangle/\mu_1$  at midpoints – which we used directly as order-parameter for  $N_f=1$  and with an additional factor of  $2^{7/4}\pi^{1/2}e^{-\gamma}\cdot\sqrt{\lambda}$  for  $N_f=2$  – as a function of the dimensionless inverse temperature  $\sigma=\mu_1\beta$  and box-length  $\lambda=\mu_1L$ .

Our aim was to give a qualitative picture of the behaviour of the Schwinger model when quantized as described above. We found that on a logarithmic temperature-scale (with  $L$  kept finite but fixed) the condensate undergoes a well-localized crossover from a fairly constant value (at low temperatures) to a value which is exponentially close to zero at sufficiently high temperature – both for  $N_f=1$  and  $N_f=2$ . For  $N_f=1$  the condensate ends up with a finite (nonzero) value after  $L\rightarrow\infty$ . For  $N_f=2$  the condensate ends up being exactly zero under  $L\rightarrow\infty$ , but the way it approaches this limiting value is rather different for fixed  $T=0$  versus fixed  $T>0$ : extremely reluctantly (i.e.  $\propto 1/\sqrt{L}$ ) in the first case versus exponentially fast in the second case. From this we concluded that it is most reasonable to include a factor of  $\sqrt{L}$  into the order parameter in case  $N_f=2$  and to define the broken quasi-phase as the set of points in parameter-space where the order-parameter exceeds half of the value it picks up when the limit  $\beta\rightarrow\infty$  is performed first and  $L\rightarrow\infty$  thereafter. The remaining points constitute the quasi-phase with quasi-restored chiral symmetry.

For  $N_f=1$  the order-parameter stays finite (i.e. nonzero) after  $L\rightarrow\infty$  for any  $T$ , and the fact that it is just exponentially close but not equal to zero for  $T\gg|e|$  confirms the statement by Dolan and Jackiw that the one-flavour system never restores the anomalously broken  $U(1)_A$ -symmetry at finite temperature [8].

For  $N_f = 2$  the order-parameter  $2^{7/4}\pi^{1/2}e^{-\gamma} \cdot \sqrt{\lambda} |\langle \psi^\dagger P_\pm \psi \rangle|/\mu_1$  vanishes under  $L \rightarrow \infty$  for any fixed nonzero temperature. Only in case  $T = 0$  the two-flavour order-parameter approaches the value 1 under  $L \rightarrow \infty$ . Thus the two-flavour analog of the l.h.s. of figure 9 looks radically different: this graph is *disconnected*, i.e. the dot at  $T=0$  (ordinate-value one) is separated from the graph for all  $T>0$  where the ordinate-value is exactly zero.

We have shown that the actual height of this “disconnected dot” is *not unique* but may take any value out of the interval  $[0, 1]$  – i.e. the *value of the order-parameter* of the two-flavour system at  $\beta = L = \infty$  *depends on the history* of the system. We have argued that this behaviour can be understood as being due to a *coexistence* of a chirally symmetric and a chirally broken phase. The relative weights the two-flavour system is giving these two states at  $\beta = L = \infty$  can be arbitrarily tuned by the way  $\beta = L = \infty$  is approached and the *two pure states* the two-flavour-system at  $\beta = L = \infty$  is composed of get *individually realized* by performing either of the two limits first. Our results confirm the picture [9] that the two-flavour Schwinger model “undergoes” a phase-transition (here without “quasi”) at  $T_c = 0$  in the sense that  $\beta = L = \infty$  may be seen as a *critical point* (for  $N_f = 2$ ).

Our rederivation has – apart from the result – nothing in common with the elegant indirect analysis by Smilga and Verbaarschot [9]: These two authors determined the scalar susceptibility in the Schwinger model with two equally massive flavours and completed the list of critical exponents at small but nonzero temperature. Their result is that this list can be understood most easily as to consist of entries which satisfy the scaling relations for a system slightly above a second order phase-transition with  $T_c = 0$ .

It is amusing to rephrase our results in the language of the usual approach where the infrared regulating and explicit chiral symmetry breaking device is the small fermion mass  $m$  rather than the inverse box-length  $1/L$ . If we make the identification  $L \leftrightarrow 1/m$ , the order-parameter at zero temperature and finite fermion mass is easily derived from (89), whereas the order-parameter at zero quark-mass but finite temperature is always zero except for  $N_f = 1$ . Thus the noncommutativity-phenomenon (77, 78) takes the form

$$\lim_{T \downarrow 0 (m \downarrow 0)} \left( \frac{\langle \psi^\dagger P_\pm \psi \rangle}{|e|^{1/N_f} m^{1-1/N_f}} \right) \propto N_f^{1/2N_f} \exp \left\{ \frac{1}{N_f} \left( \gamma - 2 \sum_{j \geq 1} (-1)^j K_0(j \sqrt{N_f} \frac{|e|}{m}) \right) \right\} \quad (81)$$

$$\lim_{m \downarrow 0 (T > 0)} \left( \frac{\langle \psi^\dagger P_\pm \psi \rangle}{|e|^{1/N_f} m^{1-1/N_f}} \right) \propto \begin{cases} \exp \left\{ \gamma - 2 \sum_{j \geq 1} K_0(j|e|/kT) \right\} & (N_f = 1) \\ 0 & (N_f \geq 2) \end{cases} \quad (82)$$

from which we learn that the Schwinger model has a phase-transition at  $T_c = 0$  for *any* number of flavours bigger than one. In particular, we see that there is nothing wrong a priori in including a factor  $L^{1-1/N_f}$  (corresponding to  $m^{-1+1/N_f}$ ) into the condensate for building the order parameter, but the result (81, 82) also shows that the dimensionless order-parameter is built in such a way as to compensate for the fact that the quasi-Goldstones of the massive Schwinger model decouple (get sterile) in the chiral limit.

So far the results for the massive Schwinger model we are aware of either rely on doing perturbation theory in the fermion mass [24] (which, given the result (77, 78) in a quantization scheme where the spatial boundary conditions take the symmetry-braking role of the fermion mass, might be dangerous) or on bosonization rules (see, e.g. [25]). While the original derivation of some of these rules was within the mass-perturbation approach [26], the rules themselves seem to be exact: Based on the bosonization approach Hetrick, Hosotani and Iso found the noncommutativity of  $m \downarrow 0$  and  $T \downarrow 0$  predicted by (81, 82) in the case of 2

and 3 massive flavours [27]. However, for the bosonization rules to be practically useful the condition  $m \ll |e|$  seems to be necessary, whereas our results are supposed to be exact for any value of  $|e|L$ .

In summary, our quantization method [15, 16, 17, 18] allows for a direct verification of a result which was obtained by Smilga and Verbaarschot through an indirect argument [9]. It is worth emphasizing that our derivation is based on conceptual grounds which are exceedingly simple: The quasi-phase diagrams are illustrations of analytical straightforward-calculations (not employing bosonization-rules) in a quantization scheme which *avoids instantons* and where the boundary conditions – besides providing a safe infrared-regulator – permanently force the system (with the exception of  $\beta=L=\infty$  for  $N_f \geq 2$ ) into a pure state.

## Acknowledgments

I would like to acknowledge the warm hospitality received at the Institute for theoretical Physics of the University of Zürich where parts of this work were done. In addition, I would like to thank A.Wipf for an earlier collaboration from which our investigations have taken benefit.

This work has been supported by the Swiss National Science Foundation (SNF).

## Appendix

Here we shall give the details for the derivation of formulas (67, 68, 72, 73).

As one concentrates on the midpoints ( $\xi = 1/2$ ), the r.h.s. of (63) takes the form

$$\begin{aligned}
(63) &= \pm \frac{e^{\pm\theta/\text{ch}(\lambda/2)}}{4\lambda} \sum_{n \in \mathbb{Z}} (-1)^n \frac{1}{\text{ch}(n\pi\tau)} \exp(-n^2\pi\tau) \cdot \\
&\quad \exp \left\{ 2 \sum_{n \geq 0} \frac{\text{cth}((2n+1)\pi\tau)}{(2n+1)} - ((2n+1) \rightarrow \sqrt{(2n+1)^2 + (\lambda/\pi)^2}) \right\} \\
&= \pm \frac{e^{\pm\theta/\text{ch}(\lambda/2)}}{4\lambda} \left( 1 + 2 \sum_{n \geq 1} (-1)^n \frac{1}{\text{ch}(n\pi\tau)} \exp(-n^2\pi\tau) \right) \cdot \\
&\quad \exp \left\{ 2 \sum_{n \geq 0} \frac{1}{(2n+1)} - \frac{1}{\sqrt{(2n+1)^2 + (\lambda/\pi)^2}} \right\} \\
&\quad \exp \left\{ 4 \sum_{n \geq 0} \sum_{m \geq 1} \frac{e^{-2m(2n+1)\pi\tau}}{(2n+1)} - ((2n+1) \rightarrow \sqrt{(2n+1)^2 + (\lambda/\pi)^2}) \right\} \\
&= \pm \frac{e^{\pm\theta/\text{ch}(\lambda/2)}}{4\lambda} \left( 1 + 2 \sum_{n \geq 1} (-1)^n \frac{1}{\text{ch}(n\pi\tau)} \exp(-n^2\pi\tau) \right) \cdot \\
&\quad \exp \left\{ 2 \left( \frac{\gamma}{2} + \frac{1}{2} \log\left(\frac{\lambda}{\pi}\right) - \sum_{j \geq 1} (-1)^j K_0(j\lambda) \right) \right\} \\
&\quad \exp \left\{ 4 \sum_{n \geq 0} \frac{1}{(2n+1)(e^{2(2n+1)\pi\tau} - 1)} - ((2n+1) \rightarrow \sqrt{(2n+1)^2 + (\lambda/\pi)^2}) \right\} \quad (83)
\end{aligned}$$

which is the result (67) quoted in subsection 4.5 and where we used [22]

$$\sum_{j \geq 0} \frac{1}{2j+1} - \frac{1}{\sqrt{(2j+1)^2 + (x/\pi)^2}} = \frac{\gamma}{2} + \frac{1}{2} \log\left(\frac{x}{\pi}\right) - \sum_{j \geq 1} (-1)^j K_0(jx) \quad (84)$$

with  $\gamma = 0.57 \dots$  the Euler gamma and  $K_0$  the modified Bessel function.

As one concentrates on the midpoints ( $\xi = 1/2$ ), the r.h.s. of (64) takes the form

$$\begin{aligned} (64) &= \pm \frac{e^{\pm\theta/\text{ch}(\lambda/2)}}{2\sigma} \sum_{m \in \mathbb{Z}} (-1)^m \frac{1}{\text{sh}(\pi(2m+1)/2\tau)} \times \\ &\quad \frac{\sum_{k \in \mathbb{Z}} e^{\pi(m+1/2)(2k+m+1/2)/\tau} (\text{erf}(\frac{(k+m+1)\sqrt{\pi}}{\sqrt{\tau}}) - \text{erf}(\frac{(k+m)\sqrt{\pi}}{\sqrt{\tau}}))}{2} \\ &\quad \exp\left\{\pi\left(\frac{1}{4\tau} - \frac{\text{th}(\lambda/2)}{\sigma}\right) + \sum_{m \geq 1} \frac{\text{th}(m\pi/2\tau)}{m} - (m \rightarrow \sqrt{m^2 + (\sigma/2\pi)^2})\right\} \\ &= \pm \frac{e^{\pm\theta/\text{ch}(\lambda/2)}}{2\sigma} \sum_{m \in \mathbb{Z}} (-1)^m \frac{1}{\text{sh}(\pi(2m+1)/2\tau)} \times \\ &\quad \frac{\sum_{k \in \mathbb{Z}} e^{\pi(m+1/2)(2k+1-m-1/2)/\tau} (\text{erf}(\frac{(1+(2k+1))\sqrt{\pi}}{2\sqrt{\tau}}) + \text{erf}(\frac{(1-(2k+1))\sqrt{\pi}}{2\sqrt{\tau}}))}{2} \\ &\quad \exp\left\{\pi\left(\frac{1}{4\tau} - \frac{\text{th}(\lambda/2)}{\sigma}\right) + \sum_{m \geq 1} \frac{1}{m} - \frac{1}{\sqrt{m^2 + (\sigma/2\pi)^2}}\right\} \cdot \\ &\quad \exp\left\{2 \sum_{m \geq 1} \sum_{n \geq 1} (-1)^n \frac{e^{-2n(m\pi/2\tau)}}{m} - (m \rightarrow \sqrt{m^2 + (\sigma/2\pi)^2})\right\} \\ &= \pm \frac{e^{\pm\theta/\text{ch}(\lambda/2)}}{\sigma} \sum_{m \geq 0} (-1)^m \frac{e^{-\pi((2m+1)^2-1)/4\tau}}{\text{sh}(\pi(2m+1)/2\tau)} \times \\ &\quad \sum_{k \geq 0} \text{ch}\left(\frac{\pi(2m+1)(2k+1)}{2\tau}\right) (\text{erf}(\frac{((2k+1)+1)\sqrt{\pi}}{2\sqrt{\tau}}) - \text{erf}(\frac{((2k+1)-1)\sqrt{\pi}}{2\sqrt{\tau}})) \cdot \\ &\quad \exp\left\{\gamma + \log\left(\frac{\sigma}{4\pi}\right) + \frac{\pi(1 - \text{th}(\lambda/2))}{\sigma} - 2 \sum_{j \geq 1} K_0(j\sigma)\right\} \cdot \\ &\quad \exp\left\{-2 \sum_{m \geq 1} \frac{1}{m(e^{m\pi/\tau} + 1)} - (m \rightarrow \sqrt{m^2 + (\sigma/2\pi)^2})\right\} \end{aligned} \quad (85)$$

which is the result (68) quoted in subsection 4.5 and where we used [22]

$$\sum_{j \geq 1} \frac{1}{j} - \frac{1}{\sqrt{j^2 + (x/\pi)^2}} = \gamma + \frac{\pi}{2x} + \log\left(\frac{x}{2\pi}\right) - 2 \sum_{j \geq 1} K_0(2jx) \quad (86)$$

with  $\gamma = 0.57 \dots$  the Euler gamma and  $K_0$  the modified Bessel function.

As one concentrates on the midpoints ( $\xi = 1/2$ ), the r.h.s. of (65) takes the form

$$(65) = \pm \frac{e^{\pm\theta/\text{ch}(\lambda/\sqrt{2})}}{4\lambda} \sum_{n \in \mathbb{Z}} (-1)^n \frac{1}{\text{ch}(n\pi\tau)} \cdot \frac{\sum_{k \in \mathbb{Z}} e^{-k^2\pi\tau - (n-k)^2\pi\tau}}{\sum_{k \in \mathbb{Z}} e^{-2k^2\pi\tau}} \cdot$$

$$\begin{aligned}
& \exp \left\{ \sum_{n \geq 0} \frac{\text{cth}((2n+1)\pi\tau)}{(2n+1)} - ((2n+1) \rightarrow \sqrt{(2n+1)^2 + 2(\lambda/\pi)^2}) \right\} \\
&= \pm \frac{e^{\pm\theta/\text{ch}(\lambda/\sqrt{2})}}{4\lambda} \sum_{n \in \mathbb{Z}} (-1)^n \frac{1}{\text{ch}(n\pi\tau)} \cdot \frac{e^{-n^2\pi\tau/2} \sum_{k \in \mathbb{Z}} \frac{e^{-(n/2-k)^2 2\pi\tau} + e^{-(n/2+k)^2 2\pi\tau}}{2}}{\sum_{k \in \mathbb{Z}} e^{-2k^2\pi\tau}} \cdot \\
& \exp \left\{ \sum_{n \geq 0} \frac{1}{(2n+1)} - \frac{1}{\sqrt{(2n+1)^2 + 2(\lambda/\pi)^2}} \right\} \\
& \exp \left\{ 2 \sum_{n \geq 0} \sum_{m \geq 1} \frac{e^{-2m(2n+1)\pi\tau}}{(2n+1)} - ((2n+1) \rightarrow \sqrt{(2n+1)^2 + 2(\lambda/\pi)^2}) \right\} \\
&= \pm \frac{e^{\pm\theta/\text{ch}(\lambda/\sqrt{2})}}{4\lambda} \left( 1 + 2 \sum_{n \geq 1} (-1)^n \frac{e^{-n^2\pi\tau/2}}{\text{ch}(n\pi\tau)} \cdot \frac{e^{-n^2\pi\tau/2} + 2 \sum_{k \geq 1} \frac{e^{-(n/2-k)^2 2\pi\tau} + e^{-(n/2+k)^2 2\pi\tau}}{2}}{1 + 2 \sum_{k \geq 1} e^{-2k^2\pi\tau}} \right) \cdot \\
& \exp \left\{ \frac{\gamma}{2} + \frac{1}{2} \log\left(\frac{\sqrt{2}\lambda}{\pi}\right) - \sum_{j \geq 1} (-1)^j K_0(j\sqrt{2}\lambda) \right\} \\
& \exp \left\{ 2 \sum_{n \geq 0} \frac{1}{(2n+1)(e^{2(2n+1)\pi\tau} - 1)} - ((2n+1) \rightarrow \sqrt{(2n+1)^2 + 2(\lambda/\pi)^2}) \right\} \tag{87}
\end{aligned}$$

which is the result (72) quoted in subsection 4.5. and where we used (84).

As one concentrates on the midpoints ( $\xi = 1/2$ ), the r.h.s. of (66) takes the form

$$\begin{aligned}
(66) &= \pm \frac{e^{\pm\theta/\text{ch}(\lambda/\sqrt{2})}}{2\sigma} \sum_{m \in \mathbb{Z}} (-1)^m \frac{1}{\text{sh}(\pi(2m+1)/2\tau)} \times \\
& \frac{\sum_{p \in \mathbb{Z}} \sum_{q \in \mathbb{Z}} \frac{1+(-1)^{p+q}}{2} e^{\pi((p+m+1/2)^2 - p^2 - q^2)/2\tau} (\text{erf}(\frac{p+m+3/2}{\sqrt{2\tau/\pi}}) - \text{erf}(\frac{p+m-1/2}{\sqrt{2\tau/\pi}}))}{2 \sum_{q \in \mathbb{Z}} e^{-\pi q^2/2\tau}} \cdot \\
& \exp \left\{ \frac{\pi}{2} \left( \frac{1}{4\tau} - \frac{\text{th}(\lambda/\sqrt{2})}{\sqrt{2}\sigma} \right) + \frac{1}{2} \sum_{m \geq 1} \frac{\text{th}(m\pi/2\tau)}{m} - (m \rightarrow \sqrt{m^2 + 2(\sigma/2\pi)^2}) \right\} \\
&= \pm \frac{e^{\pm\theta/\text{ch}(\lambda/\sqrt{2})}}{2\sigma} \sum_{m \in \mathbb{Z}} (-1)^m \frac{e^{-\pi(m+1/2)^2/2\tau}}{\text{sh}(\pi(2m+1)/2\tau)} \times \\
& \frac{\sum_{q \in \mathbb{Z}} e^{-\pi q^2/2\tau} \sum_{p \in \mathbb{Z}} \frac{1+(-1)^{p+q-m}}{2} e^{\pi(p+1/2)(m+1/2)/\tau} (\text{erf}(\frac{1+(p+1/2)}{\sqrt{2\tau/\pi}}) + \text{erf}(\frac{1-(p+1/2)}{\sqrt{2\tau/\pi}}))}{2 \sum_{q \in \mathbb{Z}} e^{-\pi q^2/2\tau}} \cdot \\
& \exp \left\{ \frac{\pi}{2} \left( \frac{1}{4\tau} - \frac{\text{th}(\lambda/\sqrt{2})}{\sqrt{2}\sigma} \right) + \frac{1}{2} \sum_{m \geq 1} \frac{1}{m} - \frac{1}{\sqrt{m^2 + 2(\sigma/2\pi)^2}} \right\} \\
& \exp \left\{ \sum_{m \geq 1} \sum_{n \geq 1} (-1)^n \frac{e^{-2n(m\pi/2\tau)}}{m} - (m \rightarrow \sqrt{m^2 + 2(\sigma/2\pi)^2}) \right\}
\end{aligned}$$

$$\begin{aligned}
&= \pm \frac{e^{\pm\theta/\text{ch}(\lambda/\sqrt{2})}}{2\sigma} \sum_{m \in \mathbb{Z}} (-1)^m \frac{e^{-\pi((2m+1)^2-1)/8\tau}}{\text{sh}(\pi(2m+1)/2\tau)} \times \\
&\quad \frac{\sum_{q \in \mathbb{Z}} e^{-\pi q^2/2\tau} \sum_{p \geq 0} \text{ch}\left(\frac{\pi(p+1/2)(m+1/2)}{\tau}\right) \left(\text{erf}\left(\frac{(p+1/2)+1}{\sqrt{2\tau/\pi}}\right) - \text{erf}\left(\frac{(p+1/2)-1}{\sqrt{2\tau/\pi}}\right)\right) +}{\sum_{q \in \mathbb{Z}} e^{-\pi q^2/2\tau} \sum_{p \geq 0} (-1)^{p+q-m} \text{sh}\left(\frac{\pi(p+1/2)(m+1/2)}{\tau}\right) \left(\text{erf}\left(\frac{(p+1/2)+1}{\sqrt{2\tau/\pi}}\right) - \text{erf}\left(\frac{(p+1/2)-1}{\sqrt{2\tau/\pi}}\right)\right)} \\
&\quad \frac{2 \sum_{q \in \mathbb{Z}} e^{-\pi q^2/2\tau}}{2 \sum_{q \in \mathbb{Z}} e^{-\pi q^2/2\tau}} \\
&\quad \exp \left\{ -\frac{\pi \text{th}(\lambda/\sqrt{2})}{2\sqrt{2}\sigma} + \frac{1}{2} \left( \gamma + \frac{\pi}{\sqrt{2}\sigma} + \log\left(\frac{\sqrt{2}\sigma}{4\pi}\right) - 2 \sum_{j \geq 1} K_0(j\sqrt{2}\sigma) \right) \right\} \\
&\quad \exp \left\{ -\sum_{m \geq 1} \frac{1}{m(e^{\pi m/\tau} + 1)} - (m \rightarrow \sqrt{m^2 + 2(\sigma/2\pi)^2}) \right\} \tag{88}
\end{aligned}$$

which is the result (73) quoted in subsection 4.5. and where we used (86).

For later use we finally mention that

$$\begin{aligned}
&\sum_{m \geq 0} (-1)^m \frac{e^{-\pi((2m+1)^2-1)/8\tau}}{\text{sh}(\pi(2m+1)/2\tau)} \times \\
&\quad \frac{\sum_{q \in \mathbb{Z}} e^{-\pi q^2/2\tau} \sum_{p \geq 0} \text{ch}\left(\frac{\pi(p+1/2)(m+1/2)}{\tau}\right) \left(\text{erf}\left(\frac{(p+1/2)+1}{\sqrt{2\tau/\pi}}\right) - \text{erf}\left(\frac{(p+1/2)-1}{\sqrt{2\tau/\pi}}\right)\right) +}{\sum_{q \in \mathbb{Z}} e^{-\pi q^2/2\tau} \sum_{p \geq 0} (-1)^{p+q-m} \text{sh}\left(\frac{\pi(p+1/2)(m+1/2)}{\tau}\right) \left(\text{erf}\left(\frac{(p+1/2)+1}{\sqrt{2\tau/\pi}}\right) - \text{erf}\left(\frac{(p+1/2)-1}{\sqrt{2\tau/\pi}}\right)\right)} \\
&\quad \frac{\sum_{q \in \mathbb{Z}} e^{-\pi q^2/2\tau}}{\sum_{q \in \mathbb{Z}} e^{-\pi q^2/2\tau}} \\
&\simeq 4 * \exp\left(-\frac{\pi}{4\tau}\right) \tag{89}
\end{aligned}$$

for  $\tau \ll 1$  and that the limit  $\tau \rightarrow \infty$  for arbitrary  $N_f$  takes the form

$$\frac{\langle \psi^\dagger P_\pm \psi \rangle}{(|e|/\sqrt{\pi})} = \frac{e^{\pm\theta/\text{ch}(\sqrt{N_f}\lambda/2)}}{4\lambda} \exp \left\{ \frac{\gamma}{N_f} + \frac{1}{N_f} \log\left(\frac{\sqrt{N_f}\lambda}{\pi}\right) - \frac{2}{N_f} \sum_{j \geq 1} (-1)^j K_0(j\sqrt{N_f}\lambda) \right\} . \tag{90}$$

## References

- [1] E.V.Shuryak: The QCD Vacuum, Hadrons and the Superdense Matter, World Scientific, Singapore (1988).
- [2] A.V.Smilga (Ed.): Continuous Advances in QCD, World Scientific, Singapore (1994).
- [3] J.Schwinger, Phys.Rev. **128**, 2425 (1962).
- [4] M.P.Fry, Phys.Rev. **D47**, 2629 (1993). C.Adam, Phys.Lett. **B363**, 79 (1995).
- [5] D.I.Diakonov, V.Petrov, Phys.Lett. **147B**, 351 (1984) and Nucl.Phys. **B245**, 259 (1984). E.Shuryak, J.Verbaarschot, Nucl.Phys. **B341**, 1 (1990) and **B410**, 55 (1993). T.Schäfer, E.Shuryak, J.Verbaarschot, Nucl. Phys. **B412**, 143 (1994). T.Schäfer, E.Shuryak, Phys.Rev. **D54**, 1099 (1996).
- [6] A.V.Smilga, Phys.Rev. **D46**, 5598 (1992). A.V.Smilga, Phys.Rev. **D49**, 5480 (1994).

- [7] S.Coleman, *Comm.Math.Phys.* **31**, 259 (1973).
- [8] L.Dolan, R.Jackiw, *Phys.Rev.* **D9**, 3320 (1974).
- [9] A.V.Smilga, J.J.M.Verbaarschot, *Phys.Rev.* **D54**,1087 (1996).
- [10] J.H.Loewenstein, J.A.Swieca, *Ann.Phys.* **68**, 172 (1961). N.K.Nielsen, B.Schroer, *Nucl.Phys.* **B120**, 62 (1977). K.D.Rothe, B.Schroer, *Phys.Rev.* **D20**, 3203 (1979). N.V. Krashnikov et al, *Phys.Lett.* **B97**, 103 (1980). R.Roskies, F.Shaposnik, *Phys.Rev.* **D23**, 558 (1981). A.K.Raina, G.Wanders, *Ann.Phys.* **132**, 404 (1981). A.Z.Capri, R. Ferrari, *Nuov.Cim.* **A62**, 273 (1981). P.Becher, *Ann.Phys.* **146**, 223 (1983).
- [11] C.Gattringer, E.Seiler, *Ann.Phys.* **233**, 97 (1994).
- [12] C.Jayewardena, *Helv.Phys.Acta* **61**, 636 (1988).
- [13] I.Sachs, A.Wipf, *Helv.Phys.Acta* **65**, 652 (1992).
- [14] T.Banks, A.Casher, *Nucl.Phys.* **B169**, 103 (1980).
- [15] A.Wipf, S.Dürr, *Nucl.Phys.* **B443**, 201 (1995).
- [16] P.Hrasko, J.Balog, *Nucl.Phys.* **B245**, 118 (1984).
- [17] S.Dürr, A.Wipf, *Ann.Phys.* **255**, 333 (1997).
- [18] H.A.Falomir, R.E.Gamboa Saravi, M.A.Muschiatti, E.V.Santangelo, J.E.Solomin, hep-th/9608101 and hep-th/9608102.
- [19] E.Merzbacher, *Quantum Mechanics*, Wiley, New York (1961).
- [20] J.S.Dowker, R.Critchley, *Phys.Rev.* **D13**, 3224. (1976). S.W.Hawking, *Commun.Math. Phys.* **55**, 133 (1977).
- [21] E.Elizalde, S.G.Odintsov, A.Romeo, A.A.Bytsenko, S.Zerbini: *Zeta Regularization Techniques with Applications*, World Scientific, Singapore (1994).
- [22] I.S.Gradshcheyn, I.M.Ryzhik: *Table of Integrals, Series and Products*, Fifth Edition, Academic Press, San Diego (1995).
- [23] M.Abramowitz, I.A.Stegun: *Handbook of Mathematical Functions*, Dover Publications, New York (1970).
- [24] C.Adam, *Ann.Phys.* **259**, 1 (1997).
- [25] S.Coleman, *Ann.Phys.* **101**, 239 (1976). A.V.Smilga, *Phys.Lett.* **B278**, 371 (1992).
- [26] S.Coleman, *Phys.Rev.* **D11**, 2088 (1975).
- [27] J.E.Hetrick, Y.Hosotani, S.Iso, *Phys.Lett.* **B350**, 92 (1995). J.E.Hetrick, Y.Hosotani, S.Iso, *Phys.Rev.* **D53**, 7255 (1996).